MICROCOPY RESOLUTION TEST CHART
NATIONAL BUREAU OF STANDARDS-1963-A

AFOSR·TR· 8 3 - 0 7 7 7
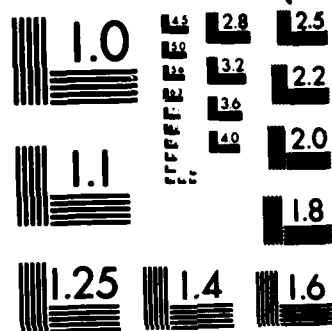
SEGMENTATION OF A HIGH RESOLUTION
URBAN SCENE USING TEXTURE OPERATORS*

Richard W. Conners, Ph.D.

Mohan M. Trivedi, Ph.D.

Charles A. Harlow, Ph.D.

DTIC
S D
OCT 5 1983
H

Approved for public release;
distribution unlimited.

September 1982

Remote Sensing and Image Processing Laboratory
Department of Electrical and Computer Engineering
Louisiana State University
Baton Rouge, LA 70803

DTIC FILE COPY

83   ?14

REPORT DOCUMENTATION PAGE	READ INSTRUCTIONS BEFORE COMPLETING FORM
1. REPORT NUMBER **AFOSR-TR- 83-0777** 2. GOVT ACCESSION NO. *AD-A133276*	3. RECIPIENT'S CATALOG NUMBER

4. TITLE (and Subtitle)	5. TYPE OF REPORT & PERIOD COVERED
SEGMENTATION OF A HIGH RESOLUTION URBAN SCENE USING TEXTURE OPERATORS	TECHNICAL
	6. PERFORMING ORG. REPORT NUMBER

7. AUTHOR(s)	8. CONTRACT OR GRANT NUMBER(s)
Richard W. Conners, Mohan M. Trivedi, and Charles A. Harlow	AFOSR-81-0112

9. PERFORMING ORGANIZATION NAME AND ADDRESS	10. PROGRAM ELEMENT, PROJECT, TASK AREA & WORK UNIT NUMBERS
Remote Sensing & Image Processing Laboratory Department of Electrical & Computer Engineering Louisiana State University, Baton Rouge LA 70803	PE61102F; 2304/A2

11. CONTROLLING OFFICE NAME AND ADDRESS	12. REPORT DATE
Mathematical & Information Sciences Directorate Air Force Office of Scientific Research Bolling AFB DC 20332	SEP 82
	13. NUMBER OF PAGES
	68

14. MONITORING AGENCY NAME & ADDRESS(If different from Controlling Office)	15. SECURITY CLASS. (of this report)
	UNCLASSIFIED
	15a. DECLASSIFICATION/DOWNGRADING SCHEDULE

16. DISTRIBUTION STATEMENT (of this Report)

Approved for public release; distribution unlimited.

17. DISTRIBUTION STATEMENT (of the abstract entered in Block 20, if different from Report)

18. SUPPLEMENTARY NOTES

19. KEY WORDS (Continue on reverse side if necessary and identify by block number)

20. ABSTRACT (Continue on reverse side if necessary and identify by block number)

This paper describes a study aimed at segmenting a high resolution black and white image of Sunnyvale, California. In this study regions were classified as belonging to any one of nine classes, residential, commercial/industrial, mobile home, water, dry land, runway/taxiway, aircraft parking, multilane highway, and vehicle parking. The classes were selected so that they directly relate to the Defense Mapping Agency's Mapping, Charting and Geodesy tangible features. To attack the problem a statistical segmentation procedure was devised. The primitive operators used to drive the segmentation are texture measures (CONTINUED)

DD ₁ FORM JAN 73 1473

ITEM #20, CONTINUED: derived from cooccurrence matrices. The segmentation procedure considers three kinds of regions at each level of the segmentation, uniform, boundary and unspecified. At every level the procedure differentiates uniform regions from boundary and unspecified regions. It then assigns a class label to the higher level regions. The boundary and unspecified regions are split to form higher level regions. The methodologies involved are mathematically developed as a series of hypothesis tests. While only a one level segmentation was performed studies are described which show the capabilities of each of these hypothesis tests. In particular an 83% correct classification was obtained in testing the labeling procedure. These studies indicate that the proposed procedure should be useful for land use classifications as well as other problems.

ABSTRACT

This paper describes a study aimed at segmenting a high resolution black and white image of Sunnyvale, California. In this study regions were classified as belonging to any one of nine classes, residential, commercial/industrial, mobile home, water, dry land, runway/taxiway, aircraft parking, multilane highway, and vehicle parking. The classes were selected so that they directly relate to the Defense Mapping Agency's Mapping, Charting and Geodesy tangible features. To attack the problem a statistical segmentation procedure was devised. The primitive operators used to drive the segmentation are texture measures derived from cooccurrence matrices. The segmentation procedure considers three kinds of regions at each level of the segmentation, uniform, boundary and unspecified. At every level the procedure differentiates uniform regions from boundary and unspecified regions. It then assigns a class label to the uniform regions. The boundary and unspecified regions are split to form higher level regions. The methodologies involved are mathematically developed as a series of hypothesis tests. While only a one level segmentation was performed studies are described which show the capabilities of each of these hypothesis tests. In particular an 83% correct classification was obtained in testing the labeling procedure. These studies indicate that the proposed procedure should be useful for land use classifications as well as other problems.

1

1. INTRODUCTION

This paper describes a study aimed at segmenting a high resolution black and white (B/W) digital image of Sunnyvale, California. This scene contained a total of 47 Defense Mapping Agency's Mapping, Charting and Geodesy (M, C & G) tangible features. The objective of the study was to segment the scene into regions which correspond to as many of these 47 M, C & G features as possible. Figure 1 shows a facsimile of the image. Table 1 shows the 9 land use classes considered in this study and their correspondence to the M, C & G features. Clearly the classes chosen do not give as detailed an image segmentation as required. The rationale for the choice of these classes is given in Section 4. Methods for achieving a more detailed segmentation using the methods presented in this paper are described in Section 3.

The time constraints of the study necessitated that readily available techniques be employed. Yet it was desired to have the methods used be as general as possible. For these reasons texture analysis methods were utilized. In particular, the spatial gray level dependence method (SGLDM) was selected because two comparison studies [1,2] have shown it to be superior, real world studies have demonstrated its capabilities [3,4,5,6,7,8,9], and perceptual psychology studies [10,11] have shown it to match a level of human perception.

In selecting the segmentation procedure the desire for generality led to the consideration of split, merge, and split and merge types of procedures [12,13]. A split type approach was the one selected. This procedure used texture measures extracted from a region R to determine whether or not R is composed entirely of one of K known classes. If R contains one of these classes then it is appropriately labeled. If not,

1

Figure 1: A facsimile of the high resolution black and white image of Sunnyvale, California.

CLASS NAME	M,C & G TANGIBLE FEATURE NAME
1. Residential Area	Houses (Single Family)
	Apartment/Hotel*
2. Mobile Home Area	Mobile Homes
3. Vehicle Parking Area	Vehicle Parking Area
	Vehicle Storage/Motor Pool
4. Aircraft Parking Area	Aircraft Parking Area/Apron
5. Runway	Runway/Taxiway
	Heliport
6. Water	Salt Pan/Evaporators
	Lake/Pond Reservoir
7. Dry Land	Mineral Pile
	Dry Land (Bare/Barren Soil/
	Non-Cultimated
	Levee/Embankment/Fill
	Crop (Cultivated)
	Deciduous Woodland
8. Multilane Highway	Multilane, Divided Highway
	(Gross Median)
	Multilane Highway
	Cloverleaf/Interchange
9. Commercial/Industrial	Fabrication Industry Building
	Scrap Yard
	Industrial Building
	Industrial Conveyor
	Industrial Rotating Crane
	Commercial Building
	Apartment/Hotel*
	Barracks
	Governmental Administration Bldg.
	Military Admin/Operations Bldg.
	School Building
	RR Station/Depot
	Airport/Airbase Control Tower
	Hangar
	Aerospace Assembly Building
	Engine Test Cell
	Wind Tunnel
	Warehouse
	Greenhouse
	Drive-In Theater Screen

Table 1. A list of nine classes and the M,C & G tangible features
combined together to compose each class. Note that a region
containing the M,C & G Apartment/Hotel feature(*) is placed in
one of two classes based upon the appearance of this region.

then R is split. The inferences regarding R are based on a series of hypothesis tests. As such the procedure is related to the uniformity predicate of Pavlidis [12].

Experiments were performed which indicate the capabilities of the segmentation procedure. The purpose of one of the experiments was to determine whether texture measures could be used to accurately classify a region into urban land use classes. For this study the nine classes in Table 1 were used. The capability of the texture measures is evidenced by a training result of 90% overall correct classification. A worst case segmentation of the scene was conducted with a 83% overall correct classification. Other experiments were performed to evaluate the mechanisms used in making the decision to split. One dealt with demonstrating the ability to identify regions containing one or more "unknown" or "unspecified" classes. Another dealt with identifying regions containing two or more "known" classes, i.e., "boundary" regions.

These experiments indicate the proposed segmentation procedure is feasible and could be useful in segmenting high resolution urban scenes. Further its generality is such that it would seemingly be applicable to a variety of problems.

2. TEXTURE ANALYSIS METHODOLOGIES

2.1 *Texture Analysis and Land Use Classification*

Many different texture analysis operators have been applied to the land use classification problem. In this section a brief review of the literature will be given in order to indicate the texture analysis methods which have been employed and the results each has yielded. Generally speaking, texture operators have been used successfully on a variety of land use problems.

One of the first attempts to use texture analysis methods for land use classification was made by Lendaris and Stanley [14]. They employed the power spectral method (PSM) to analyze a high resolution B/W aerial photograph. The two classes considered were gross manmade and nothing manmade. A 98.8% correct classification was obtained in detecting natural areas.

Galloway [15] used the gray level run length method (GLRLM) to classify 54 high resolution B/W aerial photographs. The classes considered were orchard, wood, urban, suburb, lake, marsh, swamp, railroad and scrub. The percentage of correct classification obtained for each class ranged from 83% to 100%.

Hsu [16] applied a different texture algorithm in the analysis of 7 B/W aerial photographs. This method involved the calculation of 17 texture measures from 3 x 3 or 5 x 5 windows. The classes considered were vegetation, soil, pavement, composite field 1 and 2, and composite. The best probability of correct classification obtained was 84.3%.

Mitchell and Carlton [17] made use of the max-min method to find roads,

grasslands and forests in B/W aerial photographs. Basically, the max-min method involves locating local gray level extrema along a scan line of the picture. The number of extrema of strength T or greater is a measure used in making the classifications.

A study using the SGLDM was performed by Haralick et al. [4]. The data source for the study was 1:20,000 scale B/W aerial photographs. The classes considered were old residential, new residential, lake, swamp, marsh, urban, rail and woodlands. A total of 170 samples were considered. The study yielded an 82.3% overall correct classification.

The above studies all involved reasonably high resolution B/W photography. However, texture analysis has proved useful in much coarser resolution imagery such as the 1.1 acre ground resolution data of Landsat. The texture operators applied to these data were used in conjunction with the multispectral information to yield improved classification accuracies [4,18]. Texture operators have also proved useful on higher resolution multispectral scanner (MSS) data such as aircraft MSS [19,20,21].

The studies of particular interest are those involving high resolution B/W imagery. These studies can be categorized as those where selected samples were classified and those where a segmentation of a scene was attempted. Haralick et al. [4] and Galloway [15] both classified pure samples from a selected number of classes. Neither involved the consideration of regions composed of combinations of two or more classes. On the other hand Lendaris and Stanley [14], Hsu [16], and Mitchell and Carlton [17] all attempted a segmentation. Consequently, they had to classify regions composed of combinations of classes. However the number and types of classes considered in these studies do not seem suitable for urban scene analysis. Also these studies had no provision for considering

6

more than one fixed primitive region size, i.e., no splitting or merging type procedure was attempted.

2.2 *The SGLDM Algorithm*

To defend the selection of the SGLDM, recall that this algorithm has proven useful on a variety of real world problems ranging from the analysis of human radiographs to land use classifications [1,2,3,4,5,6,7,8,13,18, 19,22]. (A complete survey of texture analysis is presented in reference 23.) Next, two comparison studies have shown the SGLDM to be a superior algorithm. One of these studies [8] compared the relative merits of four algorithms, SGLDM, GLRLM, PSM and the gray level difference method (GLDM), to do terrain type classification. The SGLDM texture measures gave the best overall classification accuracy. The other comparison study [9] evaluated the amount of texture-context information contained in the intermediate matrices of these same four algorithms. Here again the cooccurrence matrices used by the SGLDM algorithm were judged to be the best. Further it is worth noting that Mitchell et al. [17] made a preliminary comparison of the max-min method to the SGLDM. The comparison was based on the probability of correct classification obtained by applying both the max-min and the SGLDM (with the energy, entropy, correlation, local homogeneity, inertia as texture measures) to a set of texture data. The results indicated that the two methods performed about equally well. This comparison together with the fact that the max-min method is computationally less complex than the SGLDM would seemingly make it a desirable alternative. However, it is believed that the max-min method is an innately weaker algorithm. This belief is based upon the many simple textures which cannot be discriminated by the max-min algorithm. For example, Figure 2 shows two visually distinct texture pairs neither of which can be discriminated by the max-min algorithm.
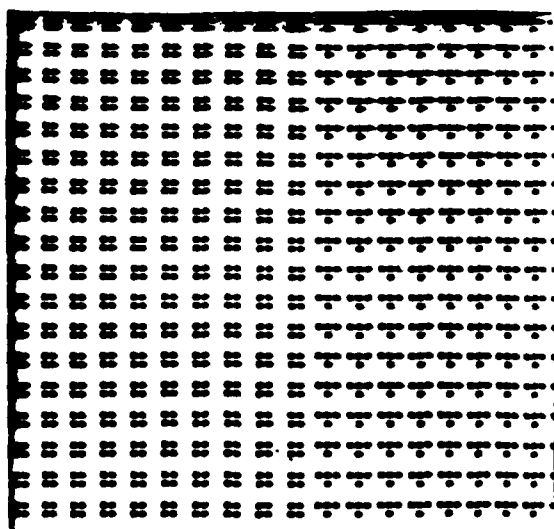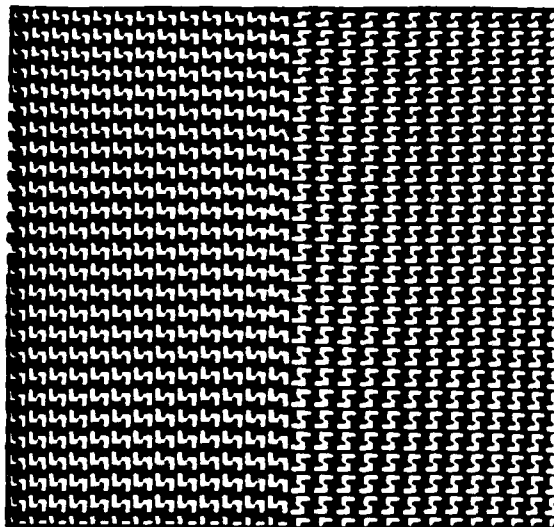
Figure 2. Two visually distinct texture pairs neither of which can be discriminated using the max-min method.

Hsu's method [16], while not having been directly compared to the SGLDM, only seem appropriate for a bottom-up approach to segmentation. Such approaches require the incorporation of world knowledge into the analysis process in order to idenitfy structures such as commercial building, parking lots, homes, etc. Incorporating such information has proved to be a difficult task one which is not generally well understood.

Finally, the Julesz conjecture [10,11] supports the use of cooccurrence matrices. It should be noted that recently a number of counterexamples to the Julesz conjecture have been reported [24,25,26,27,28]. However [29] indicates that these counterexamples can be discriminated. Hence, at present there is no known example of a visually distinct texture pair which cannot be discriminated by the cooccurrence matrices.

2.3 *Statistical and Structural Texture Analysis*

The desire has been to use cooccurrence matrices not only to discriminate texture patterns but also to be able to use them to characterize the structure in textures. In response to this motivation a model for texture was formulated based on mathematical tiling theory [30]. Later it will be shown that this model applies to the urban land use data. The system which is being developed to measure image structure using the cooccurrence matrices is called the SSA(statistical structural analysis system).

Definition 1: A *tile* T is a closed topological disk.

Definition 2: A function $\sigma:E^2 \to E^2$ is called an *isometry* or *congruence* transformation if it maps the Euclidean plane onto itself and if the function preserves distance. That is, if $\underline{x}$ and $\underline{y}$ are points in E^2 then $||\underline{x} - \underline{y}|| = ||\sigma(\underline{x}) - \sigma(\underline{y})||$.

A cooccurrence matrix $S(\delta,T) = [s(i,j,\delta,T)]$ is a matrix of estimated second-order probabilities where each element $s(i,j,\delta,T)$ is the estimated probability of going from gray level i to gray level j given the displacement vector $\delta = (\Delta x, \Delta y)$ and T, the region size and shape used to estimate the

9

probabilities. In this context T is a tile such that s(i,j,δ,T) is estimated from the restriction of the picture function g(x) to σ(T) where σ is a translation isometry. Computationally S(δ,T) is determined using the equation

$$s(i,j,\delta,T) = \frac{O\{x \mid x,\ x+\delta \in \sigma(T),\ g(x) = i,\ g(x+\delta) = j\}}{N}$$

where $N = O\{x \mid x,\ x+\delta \in T\}$ where O denotes the order of the set, i.e., the number of elements.

In what follows it is frequently convenient to consider $\delta = (\Delta x, \Delta y)$ not in a cartesian form but rather in a polar form $\delta = (d,\theta)$ where $d = \max\ [\Delta x, \Delta y]$ and $\theta = \arc \tan\ (\Delta y/\Delta x)$. In polar form d is called the intersample spacing distance and θ is called the angular orientation.

In this study six measures are computed from each matrix S(δ,T). These are:

1. Inertia

$$I(\delta,T) = \sum_{i=0}^{L-1} \sum_{j=0}^{L-1} (i - j)^2\ s(i,j,\delta,T)$$

2. Cluster Shade

$$A(\delta,T) = \sum_{i=0}^{L-1} \sum_{j=0}^{L-1} (i + j - \mu_i - \mu_j)^3\ s(i,j,\delta,T)$$

3. Cluster Prominence

$$B(\delta,T) = \sum_{i=0}^{L-1} \sum_{j=0}^{L-1} (i + j - \mu_i - \mu_j)^4\ s(i,j,\delta,T)$$

4. Local Homogeneity

$$L(\delta,T) = \sum_{i=0}^{L-1} \sum_{j=0}^{L-1} \frac{1}{1 + (i-j)^2}\ s(i,j,\delta,T)$$

5. Energy

$$E(\delta,T) = \sum_{i=0}^{L-1} \sum_{j=0}^{L-1} [s(i,j,\delta,T)]^2$$

6. Entropy

$$H(\delta,T) = -\sum_{i=0}^{L-1} \sum_{j=0}^{L-1} s(i,j,\delta,T) \log (s(i,j,\delta,T)$$

where

$$\mu_i = \sum_{i=0}^{L-1} i \sum_{j=0}^{L-1} s(i,j,\delta,T)$$

$$\mu_j = \sum_{i=0}^{L-1} \sum_{j=0}^{L-1} j \, s(i,j,\delta,T)$$

and where L is the number of gray levels in the processed image.

2.4 *Comments on the Texture Measures*

There are two places where a loss of important texture-context information can occur. The first is in going from a digital image to the cooccurrence matrices. Results reported in [2,29] together with the fact that there is no known visually distinct texture pair which cannot be discriminated by the cooccurrence matrices suggest that little texture information loss occurs here. The other place a possible loss can occur is in the transition from the matrices to the set of texture measures. It was reported in [2] that the usual set of texture measures used with the cooccurrence matrices namely, the energy, entropy, correlation, local homogeneity and inertia measures, do not contain all the important texture-context information. For example, Figure 3 shows a texture pair which can easily be discriminated using information in the cooccurrence matrices but which cannot be discriminated based on the values of the usual five texture measures computed from these matrices.
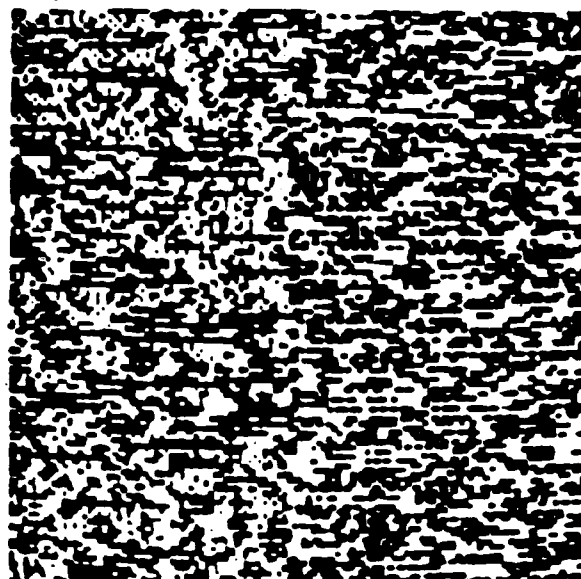
11

Figure 3. A visually distinct texture pair which can easily be discriminated based on information contained in the cooccurrence matrices but which cannot be discriminated based on the values of the energy, entropy, correlation, local homogeneity and inertia measures computed from these matrices.

Recent studies [30,31] have addressed this problem and have resulted in the definition of two new measures and an explanation of the utility of the inertia measure. The two new measures, the cluster shade and cluster prominence, are believed to gauge the perceptual concepts of uniformity and proximity [10,32]. Further it was shown that the inertia measure can be used to gauge the qualities of texture periodicity [33,34] and the texture gradient [35]. Since the inertia, cluster shade and cluster prominence are known not to be sufficient, in that a visually distinct texture pair exists which cannot be discriminated by these measures, it was decided to also include the energy, entropy and local homogeneity in the measurement set used in this study.

To see how a texture measure computed from the cooccurrence matrices can be used to determine a visual quality of a pattern consider the following example involving periodicity detection. For simplicity consider a periodic texture composed of small black squares appearing on a white background. Assume that the horizontal distance between the center of one black square to the center immediately to the right is ℓ. Further assume that this texture covers the whole plane. It can be shown [31] that the inertia measure, $I(\delta,T)$, for large enough T computed from this texture has the following properties:

i) $I(\delta,T) = 0$ for $\delta = (\ell,0°)$,

ii) $I(\delta,T) > 0$ for $\delta = (d,0°)$, $d = 1,2,\ldots,\ell-1$, and

iii) $I(\delta_n,0°) = I(\delta_{nm},0°)$ for $\delta_n = (n,0°)$, $\delta_{nm} = (md+n,0°)$ and $n,m = 1,2,\ldots$.

Consequently to find ℓ one looks for the intersample spacing distance which gives the minimum horizontal inertia value, and checks for periodicity in $I(\delta,T)$. The number ℓ then gives the period of the texture in direction θ.

The importance of this periodicity detection is that it can be used to identify a special type of unit pattern, the period parallelogram unit pattern [31]. The utility of the period parallelogram unit pattern stems from the fact that any periodic texture can be decomposed into a period parallelogram unit pattern. Further only two vectors, $\underline{a}$ and $\underline{b}$ shown in Figure 4, specify not only the size and shape of the period parallelogram unit pattern but the placement rules as well. Section 4.4 shows the importance of the period parallelogram unit pattern in the segmentation of urban scenes.
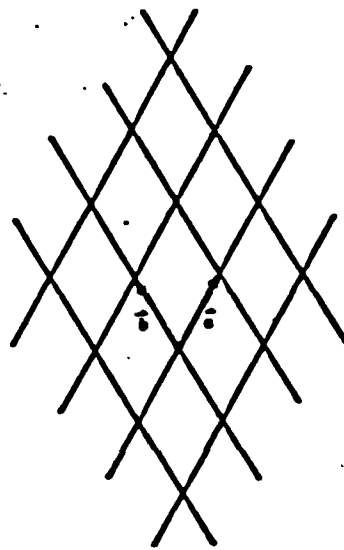
Figure 4. A period parallelogram unit pattern requires only two vectors
$\underline{a}$ and $\underline{b}$ to specify both the size and shape of the unit pattern
as well as the placement rules to arrange this pattern.

3. FRAMEWORK FOR IMAGE SEGMENTATION

The proposed segmentation procedure is an early vision system. Classically such procedures have been based upon detecting edges or detecting uniformity by examining the histogram of the gray levels [36]. The cooccurrence matrices contain edge information as well as the first-order probabilities of the gray levels. Hence measures computed from cooccurrence matrices would appear to be useful early vision operators.

Further it is desirable to have a segmentation procedure that would allow one to move back and forth between segmentation levels, verifying and reinforcing classifications without the need for semantic information. It is believed that texture operators provide a means for doing this. A texture pattern is made up of unit patterns and placement rules [31]. One can consider a commercial block as a unit pattern. The structures such as buildings and parking lots can be considered micropatterns of this unit pattern. Cast in this framework, the problem becomes one of analyzing macro and micropatterns of texture. An advantage of this approach is that one can use uniform data structures and analysis procedures in considering different levels of detail. This should provide for a better structured segmentation method.

There are basically two approaches to image segmentation. These are boundary detection and region formation [12,37,38]. Of these, region formation approaches are best suited for use with texture operators since texture operators, inherently, characterize the qualities of a region. Region formation approaches can utilize either split, merge, or split and merge techniques. A merge procedure is a bottom-up approach where small regions are combined based upon some uniformity criterion. Unfortunately, the statistical characterization of these small regions is less reliable

16

than that of larger ones. Further in complicated scenes, such as urban scenes, these small regions could belong to anyone of a large number of primitive classes such as grass, concrete, car, tree, etc. Combining these primitives to form more meaningful groups, i.e., commercial area, residential area, etc., would require a substantial reliance on semantic information.

As an example, one might decide to analyze a commercial area by first detecting edges and then linking them together to form structures of the scene. One could then perhaps consult a model to determine that these structures comprise a commercial area. A problem with this approach is that each of these subproblems is itself difficult and error prone.

A top-down procedure, such as a split procedure, seems to be best suited for use with texture operators since classification accuracies obtainable using texture analysis methods usually decrease as a function of region size. Therefore it is appropriate to use as large a region as possible and divide it as necessary. Further for an early vision system, a split procedure seems most appropriate since it begins with a few broad classes, i.e., commercial area, residential area, instead of a building, street or tree. Because of the nature of the texture algorithm as these large regions are split the texture measures computed from the smaller areas become more sensitive to finer detail. Consequently, classes whose differentiation depends on finer detail can be handled later at some higher level using smaller region size and perhaps contextual information. However, there are problems associated with initially considering a large region size. For example with large regions, it is likely that a mixture of patterns will be present. These problems are addressed in Section 3.2.

The basic steps involved in the proposed segmentation process are illustrated in Figure 5. At the first level of the segmentation the scene is initially divided into R_1 regions such that these regions cover the image. The size of the R_1 regions has been determined during the training phase when the classes at level 1 were selected. Next the appropriate texture measures are computed from the R_1 regions. These measures are also determined during the training phase when the K_1 classes are selected for level 1. Each of the R_1 regions is examined to determine if it is uniform and should be labeled with one of the K_1 class labels. If the region cannot be labeled, i.e. if it is a boundary region or it contains one or more unspecified classes, then it is passed unlabeled to the level 2 stage of processing where a new set of classes, K_2, is considered. The process should stop when all the regions are labeled. Figure 6 indicates the recursive nature of the process. Section 3.2 explains how the labeling decisions are made.

Several comments are in order. In this study only one level of segmentation was performed where the classes were labeled and the splitting criteria tested. However the formulation of the segmentation procedure will be presented in complete generality. Also the segmentation process will ultimately need to be extended to provide for a global optimization. This extension can be readily added to the methods presented.

3.1 Motivating the Statistical Segmentation Strategy

Region growing methods necessarily utilize clustering techniques [36,37,38,39]. Typically each subregion of the scene is characterized by a measurement vector $\underline{x} = [x_1, x_2, \ldots, x_n]^t$, where x_i denotes the value of measurement i. Such a vector is a point in n-dimensional Euclidean space, E^n. Intuitively, measurement vectors computed from visually similar

18

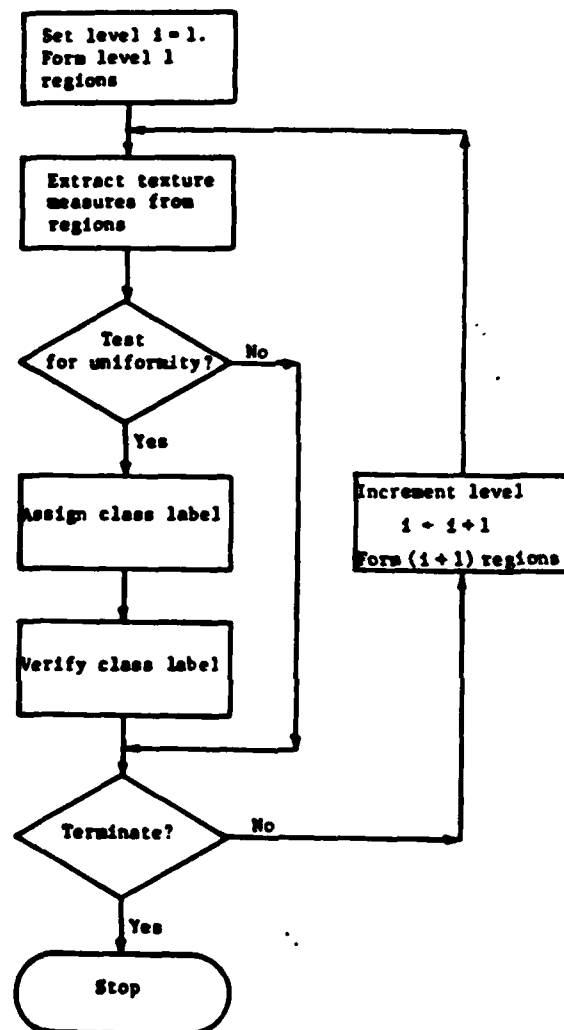Figure 5. A flowchart of the basic steps involved in the proposed segmentation procedure.
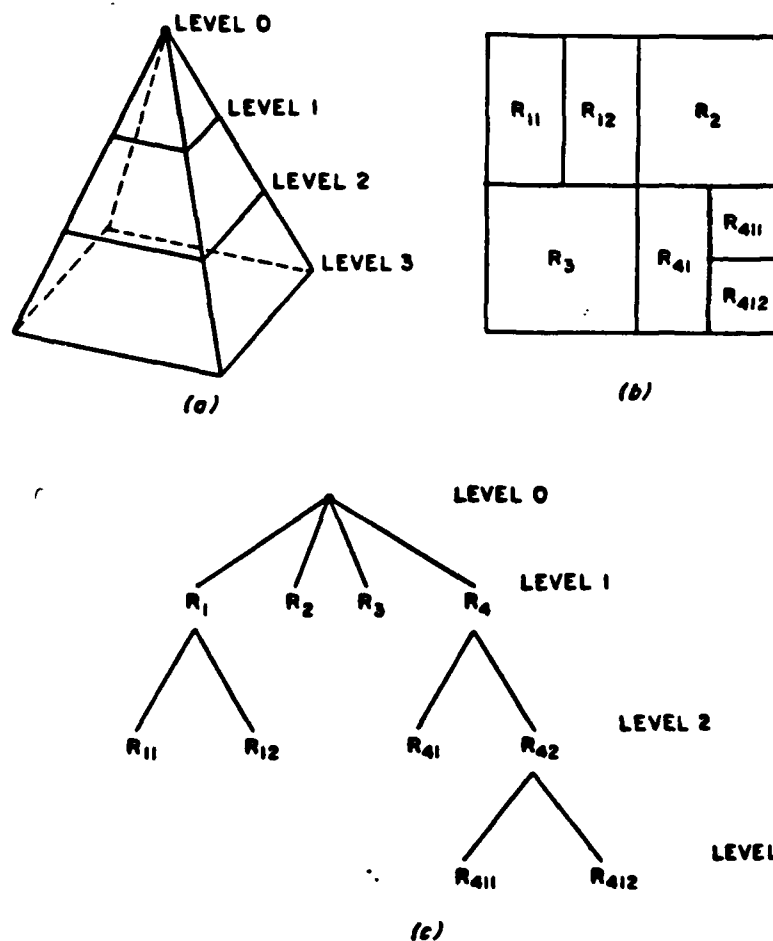
19

Figure 6. The natural pyramid structure of the segmentation. (a) An example of a three level segmentation where level 0 corresponds to the whole image, level 1 the first level of the segmentation, etc. (b) The regions formed during the segmentation. (c) A tree showing how the regions of (b) were formed.

regions should lie "close" together in E^n while measurement vectors computed from visually dissimilar regions should lie "farther" apart. Consequently, measurement vectors computed from regions containing the same class should form a cluster in E^n.

The proposed segmentation procedure attempts to incorporate the useful attributes of both supervised and unsupervised clustering approaches [39,40]. It utilizes some knowledge of the scene by allowing one to select the classes to be considered at each level of processing. This is accomplished by selecting a training set for each class at each level where it is to be considered. Thus measurement selection can be performed so that only the best measures need be used in doing the segmentation, a mode of operation allowed only by supervised procedures. The proposed procedure provides the flexibility to determine whether a region is composed in part or entirely of a class different from the K preselected classes it has been taught to recognize, a capability usually only found in unsupervised procedures. This capability to detect such "unspecified" regions is an important part of the segmentation process. The procedure also provides a mechanism for identifying regions composed of two or more of the K preselected classes, i.e., "boundary" regions. These capabilities enable it to split such unspecified and boundary regions and to examine the resulting smaller regions using different classes and different level of detail.

The proposed segmentation approach would seem somewhat similar to that presented by Chen and Pavlidis [41,42]. In this case, however, a more sophisticated multivariate formulation for the decision making is developed.

3.2 Formalizing the Concepts

To formalize the above concepts a number of definitions are useful.

Definition 3. At a particular level of the segmentation process a

region R is said to be *uniform* if it is composed entirely of only one of the K classes the procedure has been trained to recognize at that level.

Definition 4. At a particular level a region R is said to be a *boundary* region if it is composed of two or more of the K classes the procedure has been trained to recognize at that level.

Definition 5. At a particular level a region R is said to be an *unspecified* if any part of R contains a class unknown to the procedure at that level, i.e., something other than one of K classes.

The segmentation procedure requires that given a region R, the following decisions be made.

i) Determine if R is either an unspecified region or a boundary region. If it is either then split R to form higher level regions.

ii) Determine if R is a uniform region. If so, label R with one of the K possible class labels.

The capability to call R an unspecified region provides the procedure the ability to recognize an "unusual looking" region and not to force it into one of K known classes.

The required decisions can be stated as a series of hypothesis tests. For simplicity consider only two classes, ω_1 and ω_2. Given a region R, one can define the following hypotheses.

H_o: R is composed entirely of class ω_1.

H_1:   R is composed entirely of class ω_2.

H_2:   R is a mixture of both ω_1 and ω_2.

H_3:   R is composed of something other than ω_1 and/or ω_2.

22

Note that for hypothesis H_3, if any part of R contains something other than ω_1 and/or ω_2 then R is considered as not containing either ω_1 or ω_2.

Determination of the uniformity of a region involves two tests. R is uniform if either hypothesis H_o or H_1 is accepted in Tests 1 and 2. If R is uniform then Test 3 resolves the labeling.

TEST 1: H_3 versus H_o or H_1, to differentiate uniform regions from unspecified regions.

TEST 2: H_2 versus H_o or H_1, to differentiate uniform regions from boundary regions.

TEST 3: H_o versus H_1, to assign a class label to an uniform region.

Methods have been developed for performing these tests. In developing these methods an assumption was made concerning the nature of the probability density functions. The assumption not only aids in developing the tests but also allows a parametric approach be taken.

Assumption 1. Let ω_j be one of a possible K classes for a level. It is assumed that $f(\underline{x}|\omega_j)$ is normal, $N(\underline{\mu}, \Sigma_j)$, with mean $\underline{\mu}_j$ and convariance, Σ_j.

3.3 *The Multiclass Formulations of the Hypotheses Tests*

The formulations for hypothesis Tests 1,2 and 3 given above can be easily generalized to cases when more than two classes are involved. This straightforward generalization requires one to consider density functions $f(\underline{x}|\omega_j)$, $j = 1,\ldots,K$ all of which exist in the same pattern space. However, rather than using this straightforward formulation a modification will be used; one which affects the way each test will be conducted.

The motivation for the modification is based on the fact that the

23

number of training samples available limit the number of measurements that can be used. This fact stems from the Hughes' peaking phenomena [43] and Foley [44] suggests that there be at least 10 training samples available for each class for each measurement used. This restriction poses a problem in situations where there is a class with significantly fewer training samples than the other classes. In typical multiclass procedures the number of training samples available for such a class determines the maximum number of measurements which can be used to define all the classes.

Usually in an image analysis problem the quality of the measurements are such that a measure is useful in discriminating only a few of the classes. Consequently, a number of measures are required. Therefore a restriction on the number of measurements imposed by a single class would seemingly adversely effect overall performance. A better approach would be to subdivide the problem into a number of independent decisions wnere the effect of the restriction on the number of measurements will be minimized. A pairwise approach to each test accomplishes this objective.

To describe the pairwise methods used to implement the hypothesis tests the following notation will be used. Let $f_{jk}(\underline{x}_{jk}|\omega_j)$ be the class conditional density function of class ω_j for the class pair decision involving ω_j and ω_k. Assume $f_{jk}(\underline{x}_{jk}|\omega_j)$ is normal, $N(\underline{\mu}_{j,k},\Sigma_{j,k})$. To aid in understanding the notation, the subscript jk on f and $\underline{x}$ is used to indicate the density functions and measurement vector involved in the class pair ω_j, ω_k decision. The subscript j,k on $\underline{\mu}$ and Σ is an ordered pair where j indicates the class ω_j of which $\underline{\mu}$ and Σ are the mean vector and covariance matrix and k denotes the other class, ω_k, involved in the class pair decision.

24

To determine the measurement subset which defines the components of $\underline{x}_{jk}$ for each class pair a measurement selection procedure is used. The algorithm used in the study is a forward sequential search (FSS) algorithm which independently selects a subset of the available measurements to use in making each class pair decision. At the mth iteration the algorithm augments the subset selected at the $(m-1)^{st}$ iteration with another measure. This measure is the one which when combined with subset selected at the $(m-1)^{st}$ iteration gives best probability of correct classification.

3.3.1 TEST 1: Differentiating Uniform from Unispecified Regions

A region R is unspecified if either R is composed entirely of a new class, i.e., not one of the K possible; or it is composed of a combination of two or more new classes; or it is composed of a combination of one or more new classes with one or more of the K classes. In any event the distribution of $\underline{x}$ computed from unspecified regions should be different from the distributions defining the K classes. Consequently, this hypothesis test becomes merely a matter of determining whether $\underline{x}$ is a member of any of the populations of the K classes.

A standard mechanism for performing such a test is to use the Chi-squared test. In a pairwise form of this test, R is considered to be an uniform region if for at least one class ω_j

$$ t^2 = (\underline{x}_{j\ell} - \underline{\mu}_{j,\ell})^t \Sigma^{-1}_{j,\ell} (\underline{x}_{j\ell} - \underline{\mu}_{j,\ell}) < \chi^2_{\alpha;d_{j\ell}} $$

$\ell = 1,\ldots,K$, $\ell \neq j$. Otherwise consider R an unspecified region. Here $\chi^2_{\alpha;d_{j\ell}} = 100 \alpha$ percentage point of the Chi-squared distribution with $d_{j\ell}$ degrees of freedom, $\alpha = \text{Prob} (t^2 < \chi^2_{\alpha;d_{j\ell}})$, and $d_{j\ell}$ is the dimensionality of $\underline{x}_{j\ell}$ [45]. Reference 46 gives an application of such testing to texture analysis.

It should be noted that since the dimensionality of $\underline{x}_{j\ell}$ may vary from class pair to class pair, one needs a method for relating t^2, α and $\chi^2_{\alpha;d_{j\ell}}$. The interrelationship is given by

$$\alpha = \int_0^T f(t)dV = \begin{cases} 1 - \exp(-\frac{T^2}{2}) \sum_{i=1}^{d_{j\ell}/2} \frac{T^{2(i-1)}}{2^{i-1}(i-1)!} & \text{for } d_{j\ell} \text{ even} \\[2em] \sqrt{\frac{2}{\pi}} [\int_0^T \exp(-\tfrac{1}{2} r^2)dr - \exp(-\tfrac{1}{2} T^2) \sum_{i=1}^{(d_{j\ell}-1)/2} \frac{i!2^i}{(2i)!} T^{(2i-1)}] \\[1em] \hspace{6cm} \text{for } d_{j\ell} \text{ odd} \end{cases}$$

where

$$f(t) = \frac{1}{(2\pi)^{\frac{1}{2}}|\Sigma_{j,\ell}|^{d_{j\ell}/2}} e^{-\frac{1}{2}t^2}.$$

and dV is differential of volume. Note that in the above $\chi^2_{\alpha;d_{j\ell}} = T^2$.

3.2.2 TEST 2: Differentiating Uniform from Boundary Regions

A boundary region R can be composed of combinations of 2 classes, 3 classes,...,K classes. It can be argued that as the number of classes contained in a boundary region increases the more dissimilar the measures computed from this region will be from any of the K known classes. Consequently the greater the probability that such boundary regions will be detected as unspecified regions by Test 1. The more difficult problem is in differentiating uniform region from boundary regions containing only two classes. This differentiation is particularly important since as the region size gets smaller with increasing levels the basic test differentiating uniform regions from boundary regions is that involving boundary regions composed of only two classes. Therefore, the objective of Test 2 is differentiating uniform regions from such boundary regions.

To develop this test let b_{jk} denote a boundary region R composed of ω_j and ω_k. Let $\underline{x}$ be a measurement vector computed from R. Assume that $\underline{x} = \beta \underline{x}_1 + (1-\beta)\underline{x}_2$ where $\underline{x}_1$ is the measurement vector computed from the 100β percent of R which contains only class ω_j and $\underline{x}_2$ be the measurement vector computed from the $100(1-\beta)$ per cent of R which contains only class ω_j. Further assume that for b_{jk} boundary regions β is uniformly distributed $0 < \beta < 1$.

Under the above assumption it can be shown that

$$f_{jk}(\underline{x}_{jk}|b_{jk}) = \int_0^1 f_{jk}(\underline{x}_{jk}, \beta) d\beta$$

where $f_{jk}(\underline{x}_{jk})$ is the density function of $\underline{x}_{jk}$ computed from b_{jk} boundary regions and further where

$$f_{jk}(\underline{x}_{jk}, \beta) = N(\underline{\mu}_{j,k}(\beta), \Sigma_{j,k}(\beta)),$$

$$\underline{\mu}_{j,k}(\beta) = \beta \underline{\mu}_{j,k} + (1 - \beta) \underline{\mu}_{k,j},$$

and

$$\Sigma_{j,k}(\beta) = \beta^2 \Sigma_{j,k} + (1 - \beta)^2 \Sigma_{k,j}.$$

Given the above the obvious pairwise test is to call R uniform if there exist at least one k such that

$$f_{jk}(\underline{x}_{jk}|\omega_k) P(\omega_k) > f_{jk}(\underline{x}_{jk}|b_{jk}) P(b_{jk})$$

for $j = 1,\ldots,K$, $j \neq k$ where $P(b_{jk})$ denotes the a priori probability of occurrence of boundary regions composed of ω_j and ω_k. Otherwise call R a boundary region.

The development of the above test requires the estimation of the a priori probabilities, $P(b_{jk})$. These are difficult to estimate and their values can affect the test results. In addition, this test is computa-

27

tionally complex since it requires $\binom{K}{2}1$ numerical integrations to evaluate the density functions $f_{jk}(\underline{x}_{jk})$.

Because this test is computationally complex and, moreover, yields only approximate decision surfaces, it was decided to use this test only to provide intuition into developing a simplier test; one which does not require the evaluations of the density functions, $f_{jk}(\underline{x}_{jk})$. The simpler test is call R uniform if there exists at least one k such that

$$\frac{f_{jk}(\underline{x}_{jk}|\omega_j)}{f_{jk}(\underline{x}_{jk}|\omega_k)} < r$$

for $j = 1,\ldots,K$ $j \neq k$ and r, a preselected number, $0 < r < 1$. Otherwise call R an boundary region. This test is referred to as the "ratioing" test.

3.3.3 TEST 3: Labeling Uniform Regions

A pairwise Bayesian classification scheme will be used to label the uniform regions. Such a procedure is an optimal strategy for minimizing the average misclassification error for each pairwise problem [47]. The pairwise method involves solving $K(K-1)/2$ separate subproblems each involving a class pair instead of one K class problem directly. In the procedure used in this study the class conditional density functions $f_{jk}(\underline{x}_{jk}|\omega_j)$ used in making each class pair decision are assumed to be normal. Further the a priori probabilities of the classes are assumed to be equal. The results of each class pair decision are tallied using a polling function. The measurement vector is assigned to the class which rejected the vector the fewest number of times.

For a more complete description of these tests the reader is referred to [48].

4. SELECTION OF SCENE DEPENDENT PARAMETERS

In any segmentation method there are certain scene dependent para-
meters which must be input into the algorithm. For each level to be con-
sidered in the proposed segmentation algorithm the following must be
specified:

    a) the K classes, $\omega_1, \omega_2, \ldots \omega_K$, to be considered,

    b) the size of the regions, R to be used,

    c) the number of displacement vectors to be used in the computing
the cooccurrence matrices and

    d) a method for selecting the training samples from the image.

In this study only one level was considered and hence only one set
of parameters had to be selected. However, similar reasoning to that
presented should be applicable to any level. The level selected for this
study should be considered as a low level in the pyramid data structure,
see Figure 6, because of the region size used and also because of the amount
of detail present in the classes.

4.1 *Selection of the Classes for Segmentation*

Three criteria were established for selecting the classes.

1) The classes should correspond as directly as possible to the
M, C & G tangible features.

2) Each class should comprise a large enough region of the image that
an adequate training set can be selected.

3) The classes were chosen such that if R^j represents the regions of
the image labeled class ω_j, then

29

$$\bigcup_{j=1}^{K} R^j$$

should be the whole scene. Further

$$R^j \cap R^k = \phi, \ j \neq k.$$

Criterion 1,2 and 3 led to the selection of the classes in Table 1.

An important point that should be made concerning the runway, vehicle parking, aircraft parking and multilane highway classes is that all these classes are composed of the same micropatterns, namely, a large paved area surrounded by dry land. This might lead one to think that it would be difficult for texture analysis methods to discriminate them. However, one should note that there are clues that can be used by the textural analyzer. A vehicle parking area can be discriminated from the other classes because of the presence of cars parked in a regular fashion. If no cars are present the stripes used to delineate the parking places can be used to make the determination. However, if neither of these signs are present and only a concrete slab is visible then the discrimination would not be possible based solely on textural information. Similarly with the aircraft parking area, if planes are not present and parked in a regular fashion then textural information cannot be used by itself to discriminate this class. Runways and multilane highways can be discriminated because of the difference in the width of the paved area comprising them. Highways, even those with several lanes, are not usually as wide as runways or taxiways at airports. Also, the natural wear marks, i.e., tire marks, oil marks etc., are different. All these indicators can be detected by texture algorithms.

The dry land class represents a combination of five reasonably diverse M, C & G tangible features. Many of these M, C & G features made up such

a small area of the image that they could not be considered as separate classes. For example, there were only two small mineral piles and while there were 19 sited occurrences of deciduous woodland, the total area occupied was very small. Similarly, the total area of crop (cultivated) land in the scene was very small and seemed inadequate for obtaining a satisfactory training set. Finally, while there was a reasonably significant amount of levee, a decision was made not to consider levee/embankment/ fill as a separate class. Given that the mineral pile, deciduous woodland, crop (cultivated) land and levee/embankment/fill features would not be treated as separate classes, it remained to determine with which class each should be merged. The most obvious selection seemed dry land.

The most diverse class is the commercial/industrial class. It is composed of a total of twenty different M, C & G features. Each feature comprising this class did not seem to occupy enough area of the image to be considered a separate class. These twenty features were all combined into one class because no smaller groupings of them could be found which resulted in more homogeneous visual classes and which, at the same time, provided an adequate set of training samples.

Ten of the 47 M, C & G features appearing in the image defy categorization in the nine class scheme chosen. Most of these features represent "small" objects which usually occur as stand alone entities. Examples are mine shaft structure, display sign, radio/TV antenna, power transmission line etc. features. Because these features occurred so infrequently and comprised such a small area of the image, they were not considered in the segmentation.

4.2 *Selection of the Region Size*

For each level of segmentation there is a strong interrelationship between the size of the region R and the classes $\omega_1, \ldots, \omega_K$ which can be

considered. For each class ω_j the training samples for this class must be entirely composed of ω_j. The larger R the more difficult it is to find such training samples. Consequently the larger R the fewer the number, K, of classes that can be considered since each class must occupy a larger area of the scene.

The commercial/industrial class effectively established a lower bound on the region size that could be used since the "unit pattern" of the commercial/industrial class is substantially larger than the unit patterns of the other classes considered. For example, see Figures 7 and 8.

The region size selected, was 145 x 145. It was a compromise between two opposing requirements. First, one would like the size of R to be as small as possible so that a fine segmentation, i.e., the boundaries between classes can be accurately determined. Unfortunately as should be clear from Figures 7 and 8 the smaller the region size the greater the probability of misclassification. The second requirement, to have each region be labeled as accurately as possible, forces larger region sizes to be used. The size chosen was estimated by overlaying various region sizes on the image and selecting the size which appeared to be larger than the largest of the unit patterns for the various classes considered.

4.3 *Selection of the Training Samples*

Ground truth information was provided which subdivided the scene into areas corresponding to the M, C & G features. These data were translated into the nine class form using the correspondences provided in Table 1. Figure 9 shows examples of the training samples selected. Note each training sample is 145 x 145.
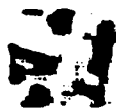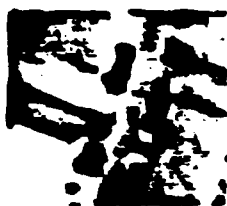
Figure 7. Examples of (a) a 50 × 50 region, (b) a 100 × 100 region, (c) a 145 × 145 region and (d) a 200 × 200 region of a commercial/industrial area.
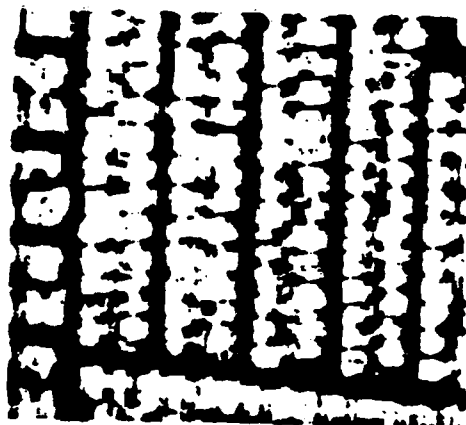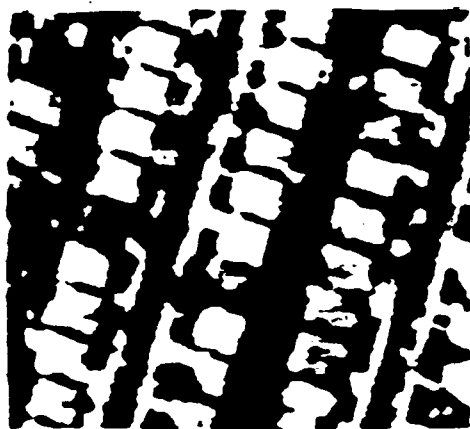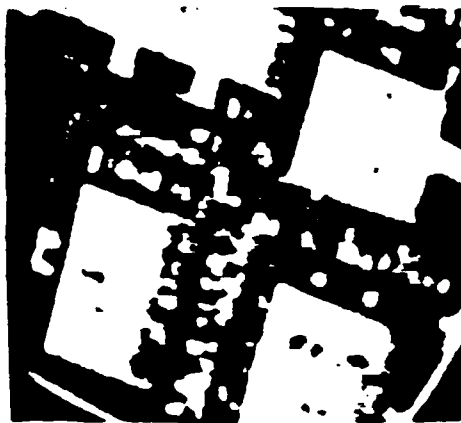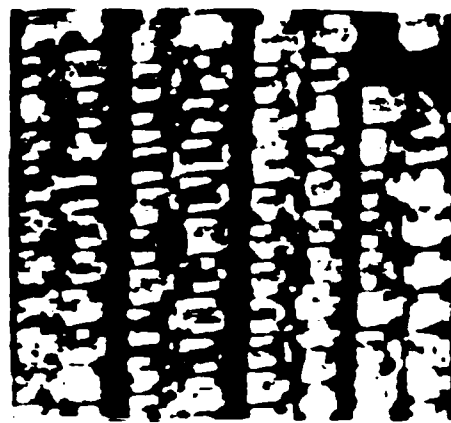
Figure 8. Examples of (a) a 50 × 50 region, (b) a 100 × 100 region, (c) a 145 × 145 region and (d) a 200 × 200 region of a mobile home area.
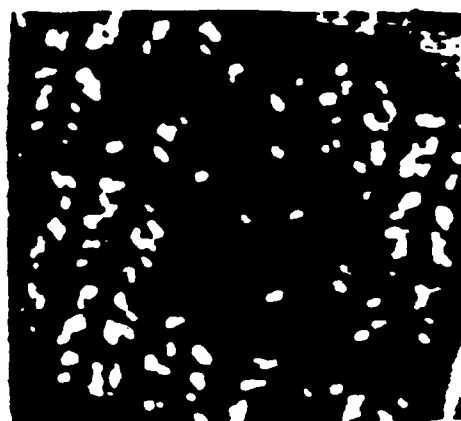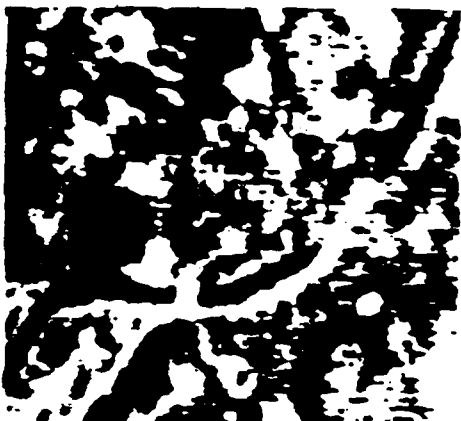
residential   commercial/industrial   mobile home
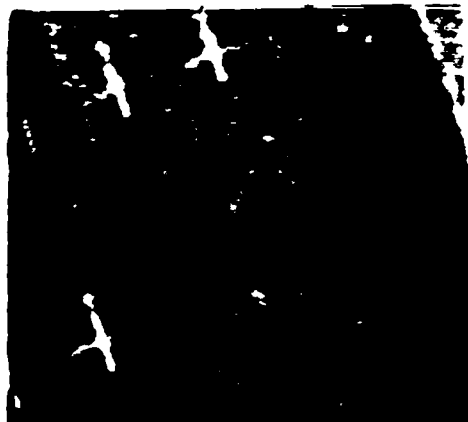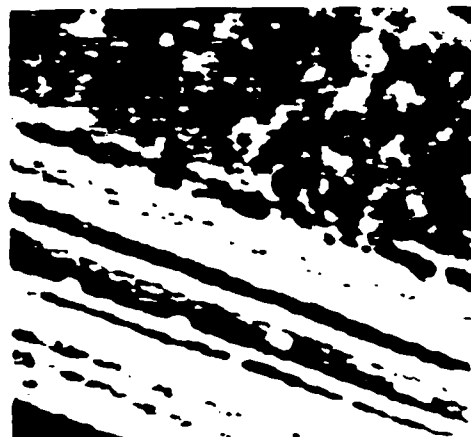
vehicle parking   dry land   water

runway/taxiway   aircraft parking   multilane highway

Figure 9. Examples of training samples for the nine classes used
in the study.

To "effectively" increase the total number of training samples, over-lapping was permitted, i.e., $S_n^j \cap S_m^j$ was not required to be ϕ where S_n^j is sample n of class ω_j and S_m^j is sample m of class ω_j. If $S_n^j \cap S_m^j \neq \phi$ then the area of the intersection was alway less than half the area of S_n^j or S_m^j, i.e., 145 x 145. An example of the overlapping is shown in Figure 10. The fact that the training sample regions overlap might seem at first glance, a bit disquieting. However, overlapping is desirable because one can not always be assured how the grid cells will be located in the testing phase of a study. Obviously in the cases where sufficient data is avail-able for training, no overlapping is required.

4.4 Selection of the Displacement Vectors

Recall the displacement vector δ is a parameter in the algorithm. For each value of δ a cooccurrence matrix, $S(\delta,T)$, is computed. Each displacement vector, $\delta = (d,\theta)$, has two components d and θ where d is the intersample spacing distance and θ is the directional orinetation. The θ parameter provides directional sensitivity and investigators have usually assumed that only four values of θ were needed, $\theta = 0°$, 45°, 90°, 135° [1,2,3,4,5,7,8,22]. Also, previous work [6,7] usually involved at most two values of d namely, d = 1,2, for a total of eight different values of δ.

Recent work [1,2,9,30,31] however, has indicated that the discriminatory power can be improved by considering more values of δ. However, from a practical point of view the number of values must be limited. The problem then is to select a relatively few δ values which will allow good discrimi-nation. Since there is little theory on the subject, of selecting the δ values, a heuristic method was employed.

First the values of θ were selected. This was done by determining the orientations of the majority of the streets appearing in the scene.
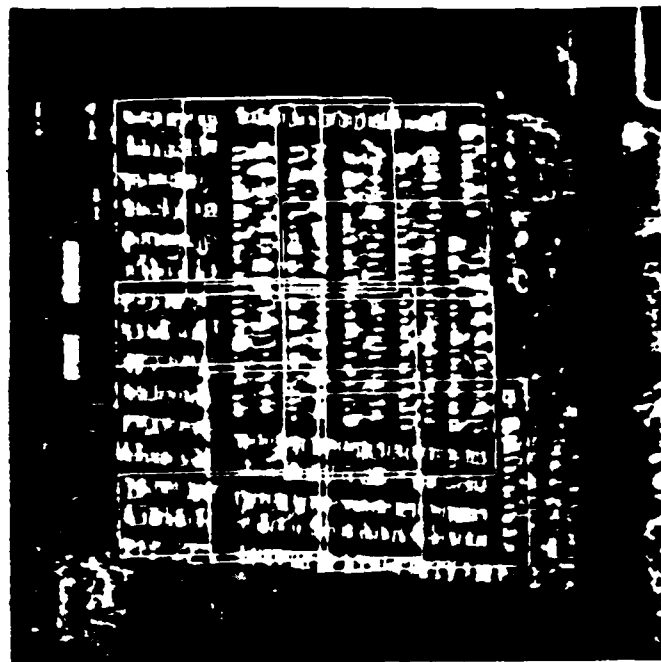
36

Figure 10. Illustrates how the training samples were
overlapped to get more training data for
the mobile home class.

It should be observed that most manmade urban structures tend to be aligned with the streets. Thus, the orientations of the streets are important. Note that the lower half and the upper right part of the Figure 1 have streets which are aligned in the 75° and 165° directions. The upper left part of the image has streets aligned in the 0° and 90° directions. Finally, the airport has runways aligned in the 19° and 109° directions. Hence, the θ's considered were 0°, 19°, 75°, 90°, 109°, and 165°. Obviously using such scene specific information as the orientation of the streets tends to limit the generality of the segmentation results.

The other component of the period parallelogram in the texture model besides the directions are the magnitudes. In order to determine if urban land use data fit this texture model representative areas from each of the nine classes were examined. Figure 11 shows a representative area selected for the residential class. From each of the representative areas the texture measures were computed for d = 1, ...,80 and for θ values which reflected the major structural character of the pattern. Usually only two θ values were considered for each of the representative regions and these θ values were usually 90° apart. This reflects the geometry of manmade structures.

Plots were generated showing the variation in the measurement values as a function of d for a given θ. Examples of two such plots for the inertia measure are shown in Figure 12. A comparison of these plots for the nine representative regions allows determination of those d values which provide good discrimination. Consider, for example, the

38
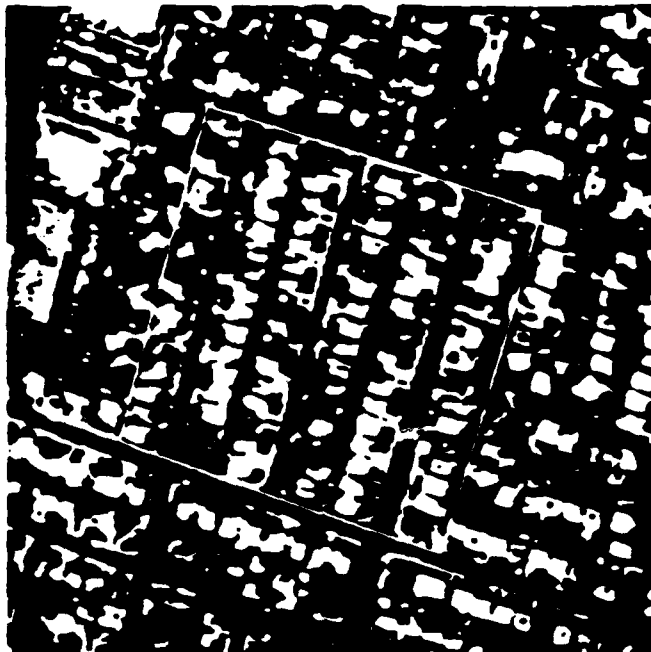
a.
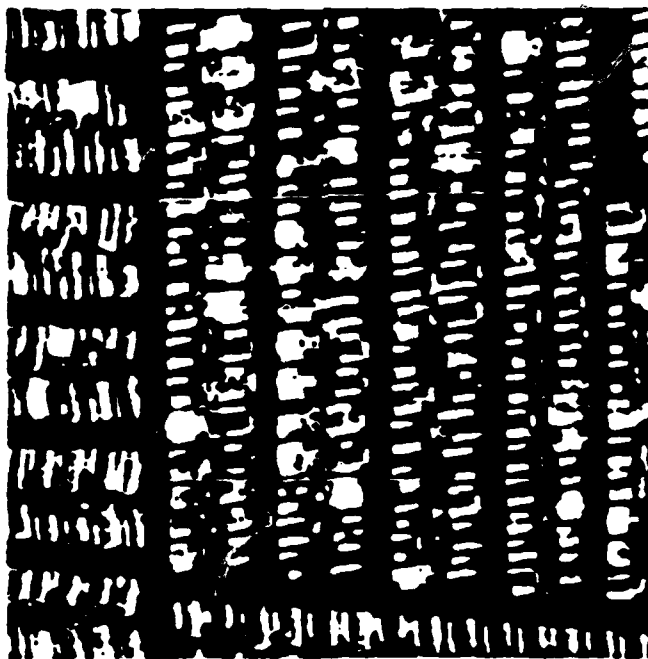
b.

Figure 11. (a) Residential area and (b) mobile home area used to compute the nominal values of the texture measurements. Note these regions were not required to be 145 x 145 but just homogeneous areas.
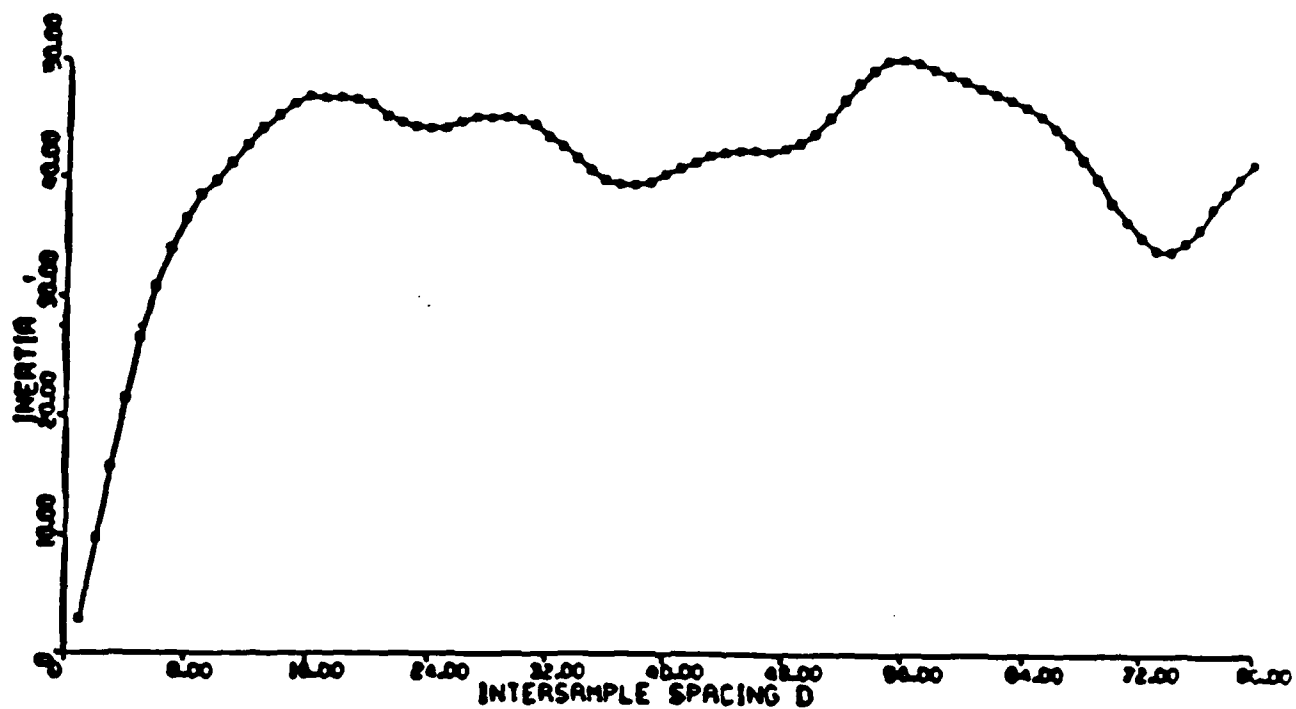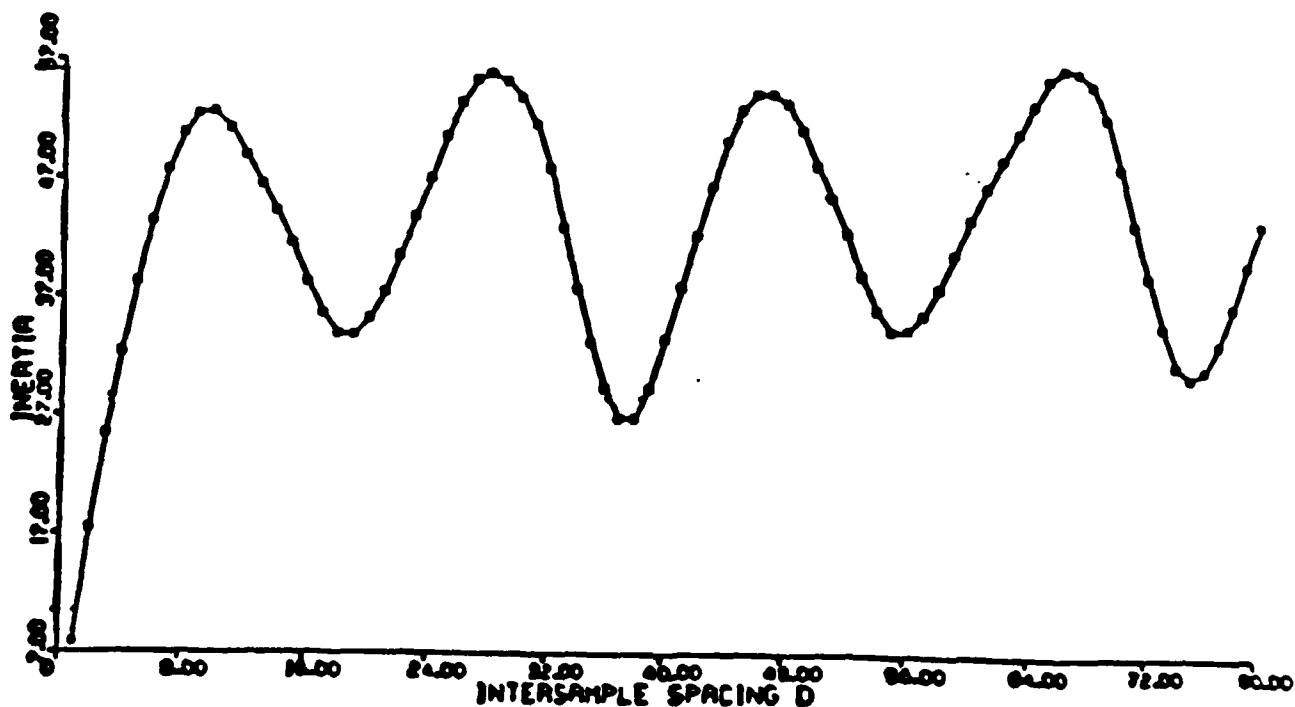
Figure 12. Plots of the inertia measure computed from the two areas
shown in Figure 11. (a) The inertia value computed from
the residential area along the θ = 165° direction.
(b) The inertia values computed from the mobile home area
along the θ = 0° direction.

plots in Figure 12(a) and 12(b). Observe that there is a significant

difference in the inertia measure values of d between 16 through 22.

Consequently, d values of 16 and 20 should provide good discrimination.

Note d values of 17,18 and 19 would also provide good discrimination

between these two classes. Similar consideration of all the plots

resulted in the selection of eight values of d, d = 1,2,4,6,8,12,16,20.

Hence the total number of δ values considered initially was 48, eight d

values and six θ values.

There are some interesting observations which can be made about the

plots in Figure 12. First, note that the local minimum occurring at d = 74

in Figure 12(a) corresponds to the distance between the streets in

Figure 11(a). Further the local minimum occurring at d = 38 corresponds

to the distance from the center of a street to the back property line of

a residential lot. Plots of the inertia measure in the 75° direction

show that the inertia measure can also be used to gauge the width of the

lots. Hence the inertia measure can determine the average lot size in

the subdivision pictured, i.e., the period parallelogram unit pattern

of the residential area. Such information could theoretically be used to

determine the area which has to be searched for objects such as cars,

driveways, etc. Similarly plots in Figure 12(b) show that the inertia

measure can be used to gauge structural information from the mobile home

area of Figure 11(b).

The last example which shows how structural information can be

gauged is the vehicle parking area shown in Figure 13. Figure 14 shows

the basic structure of this area and gives the number of pixels between

the various elements of the scene. Figure 15 shows plots of both the local

homogeneity measure and the inertia measure computed along the θ = 75°

direction. Note that the local homogeneity measure can be used to determine
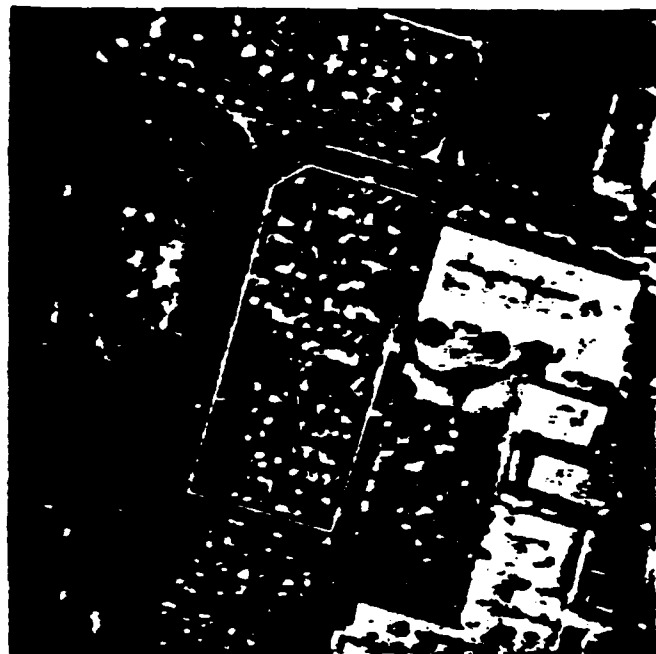
Figure 13. An example of vehicle parking area.
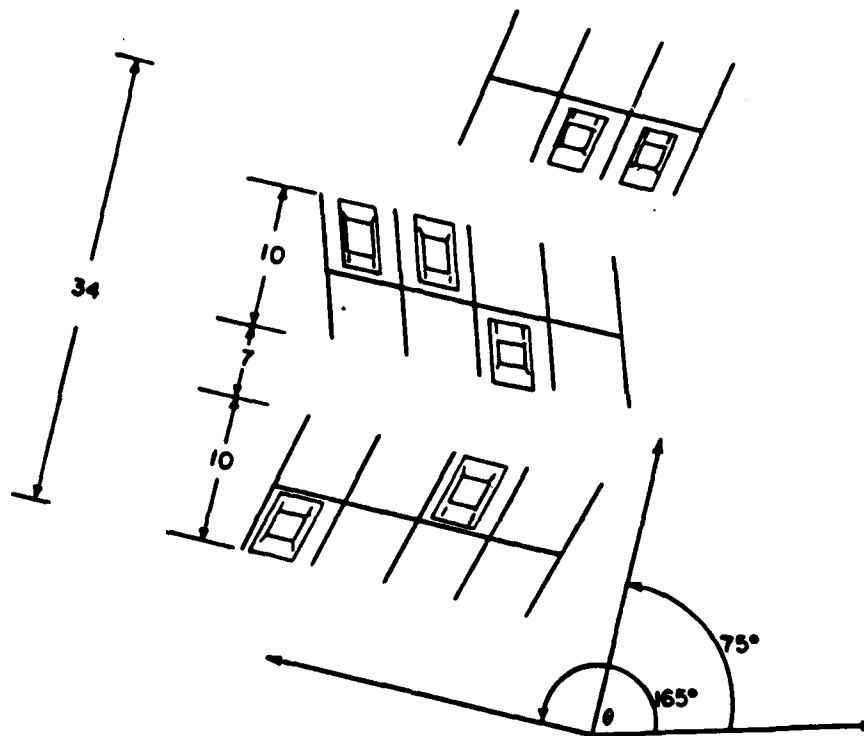
Figure 14. The structure of vehicle parking area. Also given is the number of pixels between elements of the scene.
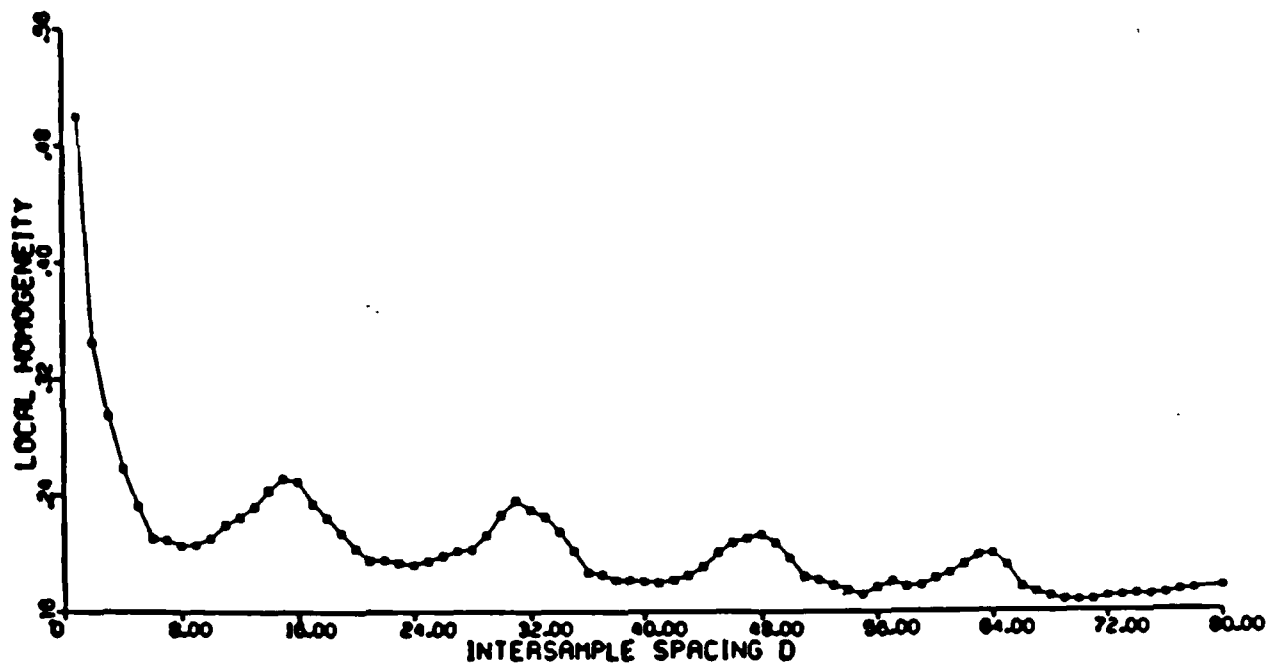
(a)
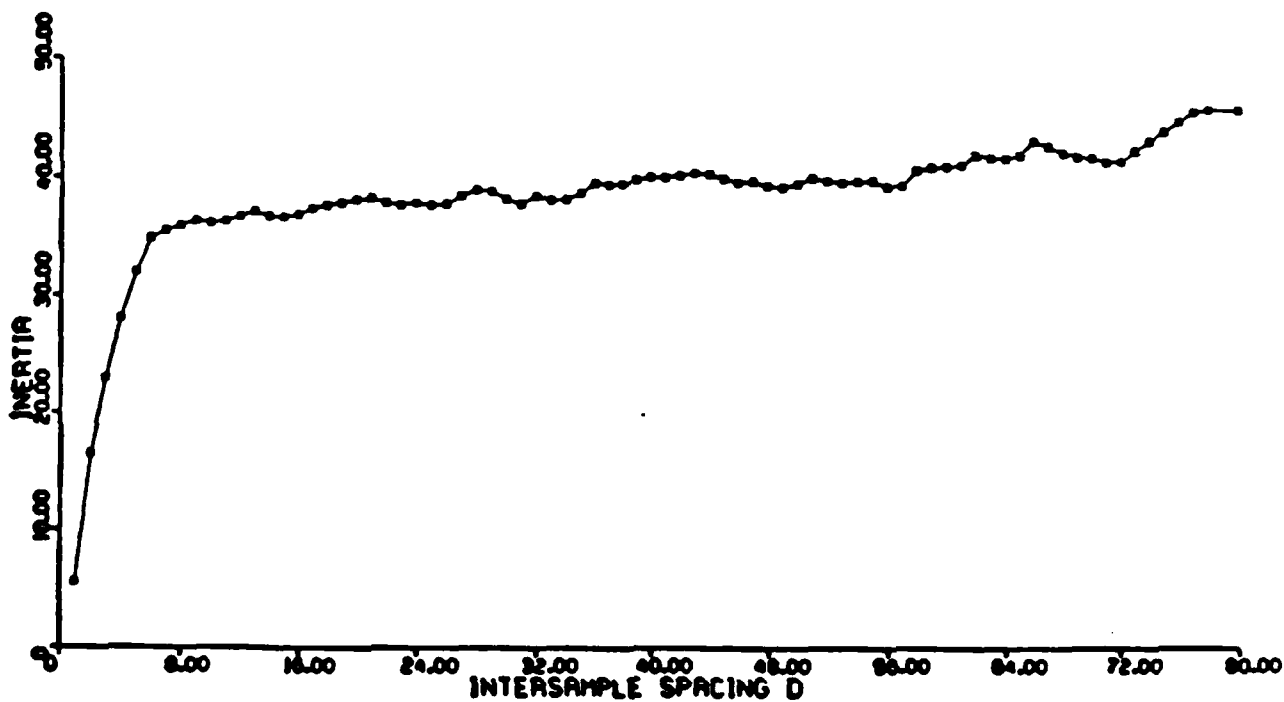
(b)

Figure 15. Plots of (a) the local homogeneity and (b) inertia measure computed from the parking area along the θ = 75° direction.

44

the distance between the rows in the parking lot while the inertia measure cannot. Further it is interesting to note that the power spectrum cannot be used to detect this structure either since the power spectrum and inertia measure are essentially equivalent [2,31].

Given the fact that the texture measures gauge visually perceivable qualities of patterns the process described above for selecting the δ values allows one to incorporate the visual differences among the classes into the segmentation process.

5. A ONE LEVEL SEGMENTATION OF THE SCENE

In this section studies are described which

  i) evaluate the capabilities of the texture measures
     to characterize the land use classes;

  ii) evaluate the capabilities of the pairwise classification
     procedure to label the uniform regions, i.e. ones which con-
     tain only one land use class; and

  iii) estimate the performance of the proposed seg-
     mentation procedure.

These studies resulted in a one level segmentation of the scene. Note

the capabilities of Chi-Squared test and ratioing tests used in differentiat-

ing uniform regions from those which should be split are given in Section 6.

5.1 *Capabilities of the Texture Measures to Characterize Land Use Classes*

The best method for evaluating the capabilities of the texture measures

is to determine how well they can discriminate the land use classes. .

Commonly the training results are used to estimate this discriminatory

power. To acquire the training results requires

  i) the extraction of the texture measures from the
     training samples;

  ii) measurement selection to obtain the measures that
     should be used to make each class pair decision;

  iii) estimation of the necessary mean vector and covariance
     matrices; and

  iv) the application of the pairwise classification pro-
     cedure to the texture measures extracted from the training
     samples.

The maximum number of measurements which could be used to make each class

pair decision was derived using the Foley criterion [44] with a minimum

of 8 samples in each class for each measure used. The measurement sele-

tion method was a forward sequential search procedure [5]. It is worth

observing that 3 of the 5 measures selected in the residential/mobile home

class pair decision involved d values of 16 and 20. Note that this agrees with the observations concerning the plots of Figure 12.

The training results for this study are given in Table 2. The percentage of overall correct classification obtained was 90%. This figure was computed by dividing the total number of correctly classified regions by the total number of training samples.

A few observations concerning the training results should be made. First, it should be noted that the commercial/industrial class and the dry land class represent the two most heterogeneous classes. That is, there are a number of visually dissimilar areas comprising each of these classes. Consider, for example, the dry land class. This class is composed of grass land, mixture of grass and trees, cultivated areas with prominent rows and areas of exposed soil with little or no grass. Similarly, the commercial/industrial class is composed of such heterogeneous possibilities as a drive-in theater screen, wind tunnels, apartments and railroad station/depot. The heterogenous make up of these classes shows itself in the training results from the fact that members of most of the other seven classes were misclassified into one or both of these classes.

Another point of interest about the training results is that the majority of the incorrect classifications were graceful misses. That is, in the majority of instances when a misclassification occurred the class in which the sample was incorrectly placed was a good second choice for placing that sample. Consider for example the residential samples that were misclassified. These samples were all labeled commercial/industrial. Residential areas look more like commercial/industrial areas than any of the rest of the classes. Further consider the misclassified mobile home samples. These samples were placed in the residential or commercial/industrial classes. Again, both of these classes represent better alternatives

47

COMPUTER CLASSIFICATION										PERCENT
	RES	COM	MH	VPK	DL	WTR	RW	APK	MHW	TOTAL	CORRECT
RES	78	5	0	0	0	0	0	0	0	83	93.98%
COM	2	297	1	1	18	0	0	0	9	328	90.55%
MH	2	3	36	0	0	0	0	0	0	41	87.80%
VPK	1	6	0	18	0	0	0	0	0	25	72.00%
DL	2	13	2	0	322	1	3	0	10	353	91.22%
WTR	0	0	0	0	1	84	0	0	0	85	98.82%
RW	0	2	0	0	6	0	70	0	0	78	89.74%
APK	0	2	0	0	1	0	0	18	0	21	85.71%
MHW	0	13	1	0	8	0	0	0	99	121	81.82%
TOTAL	85	341	40	19	356	85	73	18	118	1135	
OVERALL PERCENTAGE CORRECT CLASSIFICATION											90.04%

RES - Residential

COM - Commercial/Industrial

MH - Mobil Home

VPK - Vehicle Parking Area

DL - Dry Land

WTR - Water

RW - Runway/Taxiway

APK - Aircraft Parking

MHW - Multilane Highway

Table 2. The results obtained by classifying the
training samples. The training results
gave an 90% overall correct classification.

than any of the other classes. Also the vast majority of the misclassified
vehicle parking area samples were called commercial/industrial area samples.
Note that many of the commercial/industrial samples have large parking areas
contained in them.

Also consider the confusion between the commercial/industrial class
and the dry land class. As was stated earlier both the commercial/indus-
trial and dry land classes are heterogeneous in structure. Further, almost
every class has samples which are misclassified into one of these two classes.
The confusion between these two classes seems to be based on a similar
structure. Many of the commercial/industrial training samples have one or
more buildings surrounded by a large grassy area. Evidentially, the methods
employed have trouble discriminating areas of bare soil surrounded by grass
from buildings surrounded by grass.

Finally both the dry land class and commercial/industrial class are
confused with the multilane highway class. To explain this confusion it
should be observed that a 145 x 145 sample of multilane highway must contain
things other than a multilane highway. In the majority of the training
samples of multilane highway the other objects in the 145 x 145 areas
were either commercial/industrial areas and/or dry land.

These results are encouraging. Even though some misses occur
they indicate that texture measures can be used to characterize compli-
cated land use classes.

5.2 *Capabilities of the Pairwise Classification Procedure*

A procedure which seems appropriate for evaluating the classification scheme is to partition the image into regions as though a segmentation were to be performed and then classify only those regions which are uniform. In this case the regions are created by overlaying a 145 x 145 square grid on the image as shown in Figure 16. The resulting 1156 regions include 680 which have more than 90% of their area composed of one of the nine classes. In the study the definition of uniformity was relaxed to assure an adequate number of samples.

The results of applying the pairwise classification scheme to the 680 regions are shown in Table 3. Observe that these results are comparable to the training results given in Table 2 with the most significant difference being only 8% below tne training results. In making this comparison it is important to point out that seldom if ever did a training sample coincide with one of the 680 regions considered. Further it should be observed that three classes, namely, vehicle parking, runway/taxiway and aircraft parking, have higher percentages of correct classification than those achieved during training. This anomaly can be explained for the vehicle parking and aircraft parking classes by noting in Table 3 the small number of samples representing these two classes. To explain the discrepency for the runway/taxiway class note the fact that the positioning of the paved runway area within the 145 x 145 sample region will affect the values of the texture measures. Ideally one would like the runway to pass through the center of the region. However to adequately train the procedure to recognize this class, samples reflecting less than ideal conditions were included.
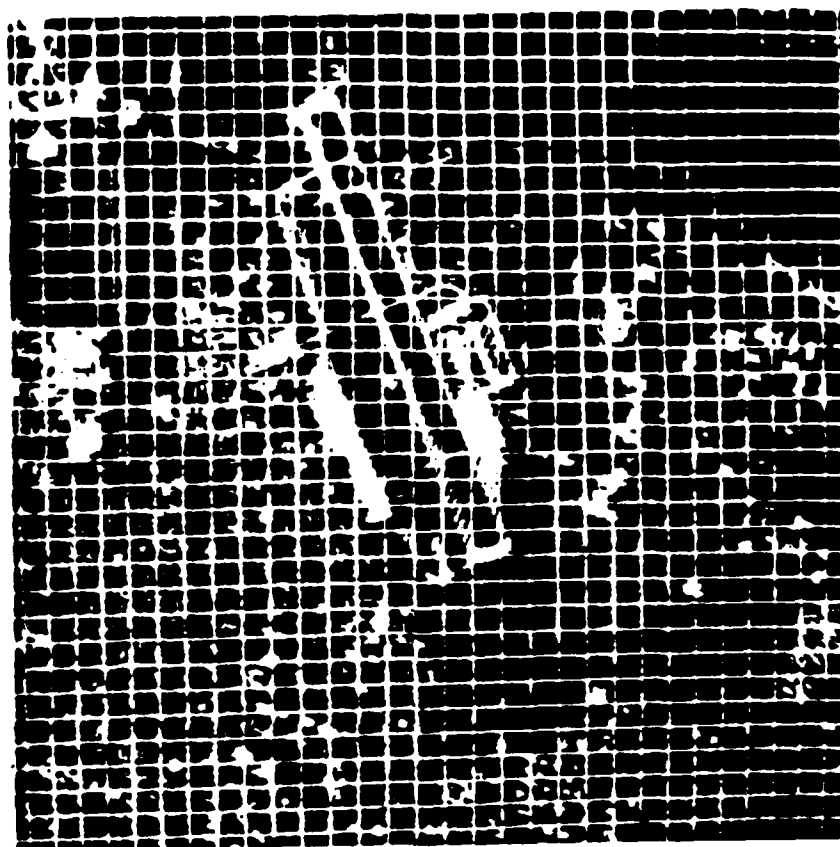
Figure 16: The square grid used to segment the Sunnyvale scene.

	COMPUTER CLASSIFICATION										PERCENT CORRECT
	RES	COM	MH	VPK	DL	WTR	RW	APK	MHW	TOTAL	
RES	28	5	0	0	0	0	0	0	0	33	87.9%
COM	5	148	1	0	6	0	5	0	8	174	85.06%
MH	0	0	6	0	0	0	0	0	1	7	85.7%
VPK	0	1	0	5	0	0	0	0	0	6	83.0%
DL	2	30	1	0	232	2	6	2	4	279	83.2%
WTR	0	1	0	0	4	88	2	0	0	95	92.6%
RW	0	0	0	0	1	0	40	0	0	41	97.6%
APK	0	0	0	0	0	0	0	5	0	5	100.%
MHW	0	6	0	0	1	0	0	0	33	40	82.5%
TOTAL	35	191	8	5	246	90	53	7	46	680	

(left axis label: VERIFIED CLASSIFICATION)

OVERALL PERCENTAGE CORRECT CLASSIFICATION	86.0%

RES - Residential

COM - Commercial/Industrial

MH - Mobil Home

UPK - Vehicle Parking Area

DL - Dry Land

WTR - Water

RW - Runway/Taxiway

APK - Aircraft Parking

MHW - Multilane Highway

Table 3. The results obtained by applying the pairwise classification scheme to 680 uniform regions of the image.

52

Consequently the difference in classification accuracies is attributable to the good runway sample region alignment occurring just by chance in this study.

Finally it should be observed that the misclassifications shown in Table 3 are very similar to those given in Table 2. The only exception being the five commercial/industrial samples which were misclassified in runway/taxiway class. To explain this note that four of five areas misclassified in this manner involved large hangars. According to Table 1 hangars are a part of the commercial/industrial class. Yet the large hangars involved in misclassifications look nothing like the commercial/industiral samples included in the training set for this class. This fact together with the visual similarity of regions containing hangars to those containing a runway explains the confusion. This can be observed from Figure 17.

5.3 A Segmentation of the Scene

Practically speaking in any automatic segmentation procedure there is a level, say level i, at which a labeling of every remaining region must be forced. Usually the percentage of the regions which are unspecified and boundary decreases with increasing i since the smaller the regions R, the more of them that will fall into areas composed of a single class. Admittedly there are mitigating factors, but a reasonable estimate of the lower bound on the performance of a segmentation can be derived by forcing a label on the regions at the lowest possible level, level 1. This follows from the fact that the percentage of unspecified and boundary regions will be maximum at this level. Such a lower bound will be estimated in this section. The data used to establish this lower bound are the 1156 145 x 145 regions shown in Figure 16.

Figure 17. The visual similarity between a region containing
a large hangar and one containing a portion of a
runway/taxiway. (a) The region containing the
hangar. (b) The region containing a runway/taxiway.

In forcing a label on these regions, a difficulty that is immediately encountered relates to establishing ground truth. For example, it is possible for some of these regions to contain multiple land use classes. To avoid any possible ambiguity rules were formulated for scoring the segmentation. Let R be a 145 x 145 square in question. Further let ω_j represent class j and $A(\omega_j)$ represent the area of R occupied by class ω_j. Then the scoring rules are as follows:

1. If R contains n classes, say $\omega_1,\ldots,\omega_n$, and if $A(\omega_j) \gg A(\omega_k)$ for all k such that $1 \leq k \leq n$, $k \neq j$, then the correct labeling of R is assumed to be ω_j.

2. If R contains n classes, say $\omega_1,\ldots,\omega_n$, and if there are m classes, say $\omega_1,\omega_2,\ldots,\omega_m$, such that $A(\omega_1) \simeq \ldots \simeq A(\omega_m)$ and further that $A(\omega_j) > A(\omega_k)$, $1 \leq j \leq m$, $m \leq k \leq n$, then the correct labeling is assumed to be anyone of the ω_j, $1 \leq j \leq m$.

The results obtained by pairwise classification procedure to label all the 1156 regions is given in Table 4. In examining these results it is again important to note that seldom if ever did a training sample coincide with one of the regions shown in Figure 16. The overall percentage of correct classification is about 83%.

As will be observed six of the nine classes have good classification accuracies, ones which compare favorably to those obtained when only uniform regions are considered (Table 3). However, three of the classes, namely, mobile home, vehicle parking and aircraft parking, do not. To explain these low classification accuracies it is important to note that when only uniform regions are considered these classes have high probabilities of correct classification. Given that each of these classes compose only a

	COMPUTER CLASSIFICATION										PERCENT
	RES	COM	MH	VPK	DL	WTR	RW	APK	MHW	TOTAL	CORRECT
RES	43	19	0	0	0	0	0	0	4	66	65.2%
COM	6	298	1	0	9	0	5	1	14	334	89.2%
MH	0	5	6	0	0	0	0	0	1	12	50.0%
VPK	0	13	0	8	0	0	0	0	1	22	36.4%
DL	2	44	1	0	378	2	12	6	10	455	83.1%
WTR	0	3	0	0	6	88	7	1	0	105	83.8%
RW	0	0	0	0	1	0	68	0	0	69	98.6%
APK	0	1	0	0	3	0	6	9	0	19	47.4%
MHW	0	9	0	1	1	0	1	0	62	74	83.8%
TOTAL	51	392	8	9	398	90	99	17	92	1156	
OVERALL PERCENTAGE CORRECT CLASSIFICATION											83.4%

(Left vertical axis label: VERIFIED CLASSIFICATION)

RES - Residential

COM - Commercial/Industrial

MH - Mobil Home

UPK - Vehicle Parking Area

DL - Dry Land

WTR - Water

RW - Runway/Taxiway

APK - Aircraft Parking

MHW - Multilane Highway

Table 4.   The results obtained when the image was segmented. It should be noted that few if any of the regions used in the segmentation exactly corresponded to the regions comprising the training set.

small percentage of the whole scene the obvious explanation for these poor results is that most of the regions misclassified were actually boundary regions. An examination of the data proves this explanation to be correct.

The percentage of correct classification of the other classes seemed acceptable. As will be observed the algorithm failed gracefully on a majority of the misclassified samples. Consider the residential class. The majority of the misclassified residential samples were labeled as commercial/industrial. Clearly if a residential area is to be missed, the commercial/industrial class is the one which most closely resembles the residential class.

The vast majority of the misclassified commercial/industrial samples were called either residential, dry land or multilane highway. Similarly, the vast majority of the misclassified dry land samples were called commercial/industrial.

This leads one to the water class. As will be observed from Table 4 some water samples are mislabeled as commercial/industrial, dry land, runway and aircraft parking. These are clearly very bad misses. However, there is a mitigating factor. All the water samples which were misclassified into either the commercial/industrial class, the runway/taxiway class, or the aircraft parking class contained a levee, i.e., an unspecified class, since none of the training samples for any of the classes contained a levee. Finally some of the confusion between the water class and the dry land class seems to be caused by mixtures of dry land and water. Water samples which contained only reasonably small areas of dry land were consistently called dry land by the algorithm.

The runway class was very accurately classified with only two of the 68 samples being misclassified as dry land. The multilane highway class

57

had samples misclassified as commercial/industrial, residential and mobile home. It is interesting to note that each of the multilane highway training samples contained areas from these three classes and dry land. However, only the commercial/industrial, residential and mobile home areas contained structures which could markedly affect the texture measures ability to detect the presence of a major road.

6. EVALUATING THE SPLITTING CRITERIA

Recall that the splitting criteria involves two tests, the Chi-Squared test and the ratioing test. The Chi-squared test was formulated primarily to differentiate uniform regions from unspecified regions whereas ratioing was primarily formulated to differentiate uniform regions from boundary regions. In this section studies aimed at evaluating these tests will be briefly described.

6.1 Evaluating the Capabilities of Chi-Squared Test

The data used to evaluate Chi-Squared test were taken from a square area in the extreme upper right hand corner of the image. This area contained 144 regions and comprised the last 12 elements of the first 12 rows of the grid given in Figure 16. This area was selected because it contained a levee and a land/water boundary. The levee is of interest because while being a part of the dry land class any 145 x 145 region containing a levee must necessarily contain water. Also the training set for the dry land class contained no levee samples. Hence the segmentation procedure should call such regions unspecified. The presence of the land/water boundary could be used to determine whether Chi-squared test could be used to find boundary regions.

The results of applying a simplified version of the Chi-squared test to the 144 regions is summarized in Table 5. The first row of this table shows how the 53 verified unspecified regions were handled by the segmentation procedure. Observe that 44 (83%) of these were correctly identified as being unspecified by the Chi-squared test. Of the 9 .regions which were mistakenly judged as being uniform, 7 of these were correctly classified by the pairwise classifier.

59

		COMPUTER RESULTS			
		1-Unspecified or 1-Boundary regions as identified by Chi-Squared test	Regions identified as 1-Uniform by the pairwise classifier		Total number of regions
			Correctly classified	Incorrectly classified	
VERIFIED CATEGORIES	1-Unspecified regions	44	7	2	53
	1-Boundary regions	11	17	2	30
	1-Uniform regions classified using pairwise classifier — 1-Uniform regions correctly classified	6	55	0	61
	1-Uniform regions incorrectly classified	0	0	0	0

Table 5: A summary of the results obtained by applying the simplified form of the Chi-squared test to the 144 regions contained in a square area in the extreme upper right hand side of the scene.

60

The second row of Table 5 shows how the verified boundary regions were handled. Observe that the Chi-squared test correctly identified 11 (37%) of the 30 regions as boundary regions. Of the 19 regions which were not identified as boundary regions by the Chi-squared test, 17 (89%) of these were labeled by the pairwise classifier as belonging to one of their major constituent classes. Therefore, only 2 out of 30 samples can be viewed as incorrectly labeled. It should be noted that the Chi-squared test is specifically derived to differentiate unspecified regions from uniform regions and the correct differentiation of boundary regions from uniform regions is really a secondary consideration for this test.

The third row corresponds to those verified uniform which were correctly labeled as being a member of one of K classes by the Chi-squared test. The fourth row corresponds to those verified uniform which were incorrectly labeled by the Chi-squared test. Observe that only 6 (10%) of the correctly labeled uniform regions were called unspecified by the test.

6.2 Evaluating the Capabilities of the Ratioing Test

The results acquired by applying the simplified version of the ratioing test to the 102 regions is given in Table 6. Also shown is the results of applying the the Chi-squared test with α = .95 and the pairwise classification procedure to these same 102 samples. The first row shows how the 65 verified boundary regions were handled. Observe that the ratioing test alone could identify 27 of these regions. In all the ratioing test identified 40 of the 65 regions. The Chi-squared test aided by detecting 10 more. Thus in combination the two tests detected 77% of boundary regions.

The second and third rows show how verified uniform regions, both those which were correctly and incorrectly classified by the pairwise classifier were treated. Observe that the ratioing test mistakenly called

61

COMPUTER RESULTS

VERIFIED CATEGORIES		1-Boundary regions				Regions identified as 1-Uniform by the pairwise classifier		Total number of regions
		Identified by Chi-Squared test	Identified by ratioing test	Identified by both Chi-Squared and ratioing tests	Total number of 1-Boundary regions identified	Correctly classified	Incorrectly classified	
1-Boundary regions		10	27	13	50	13	2	65
1-Uniform regions classified using pairwise classifier	1-Uniform regions correctly classified	11	4	3	18	11	0	29
	1-Uniform regions incorrectly classified	1	3	2	6	0	2	8

Table 6 : A summary of the results obtained by applying the simplified forms of the ratioing test and the Chi-squared test to 102 regions. Note that the table also indicates the classification results obtained by the pairwise classifier for the 102 regions.

7 (24%) of these regions boundary region. Further the Chi-squared test incorrectly labeled an additional 11 (38%). The poor performance of the Chi-squared test in this case is probably a result of a suboptimal choice of α.

On the third row observe that of the 8 incorrectly labeled uniforms by the classifier 6 (75%) regions were identified as boundary regions.

7. SUMMARY AND CONCLUSIONS

This paper described a study aimed at segmenting a high resolution urban scene. To accomplish this objective a statistical segmentation procedure was developed; one whose primitive operators were SGLDM texture measures. The procedure is an early vision system based on a split type algorithm. It considers three types of regions at each level of the segmentation, uniform, boundary and unspecified. The procedure is based on three hypothesis tests. Experiments were performed which indicate the utility of the methodologies employed. In particular a training result of 90% overall correct classification for the nine classes considered confirms the ability of the texture algorithm to characterize land use classes. Further an approximate lower bound of 83% correct classification was established on the performance of the segmentation procedure in independent testing samples. Finally the performance of the tests associated with the decision to split a region were evaluated. The results show that these tests performed well in making a split decision. The results obtained substantiate the use of texture operators to segment complicated urban scenes.

As stated previously the segmentation procedure was not completely implemented in that multiple levels could not be considered. A further study is required to consider this case. Also, methods to incorporate more world knowledge need be investigated. Finally methods for improving the measurement selection algorithm should be studied since the algorithm used considers only the ability of a measure to correctly classify uniform regions.

REFERENCES

1. Weszka, J., C. Dyer and A. Rosenfeld, "A Comparative Study of Texture Measures for Terrain Classification," IEEE Transactions on Systems, Man, and Cybernetics, Vol. SMC-6, No. 4, April 1976, pp. 269-285.

2. Conners, R. W., and C. A. Harlow, "A Theoretical Comparison of Texture Algorithms," IEEE Transactions on Pattern Analysis and Machine Intelligence, Vol. PAMI-2, No. 3, May 1980, pp. 204-222.

3. Haralick, R. M. and K. Shanmugam, "Computer Classification of Reservoir Sandstones," IEEE Transactions on Geoscience Electronics, Vol. GE-11, No. 14, October 1973, pp. 171-177.

4. Haralick, R. M., K. Shanmugam, and Its'Hak Dinstein, "Textural Features for Image Classification," IEEE Transactions on Systems, Man, and Cybernetics, Vol. SMC-3, No. 6, November 1973, pp. 610-621.

5. Ausherman, D. A., "Texture Discrimination Within Digital Imagery," Ph.D. Dissertation, University of Missouri, Columbia, December 1972.

6. Kruger, R. P., W. B. Thompson, and A. F. Turner, "Computer Diagnosis of Pneumoconiosis," IEEE Transactions on Systems, Man, and Cybernetics, Vol. SMC-4, No. 1., January 1974, pp. 40-49.

7. Hall, E. L., R. P. Kruger, and F. A. Turner, "An Optical-Digital System for Automatic Processing of Chest X-Rays," Optical Engineering, Vol. 13, No. 3, May/June 1974, pp. 250-257.

8. Darling, E. M. and R. D. Joseph, "Pattern Recognition From Satellite Altitudes," IEEE Transactions on Systems Science and Cybernetics, Vol. SSC-4, No. 1, March 1968, pp. 38-47.

9. Tully, R. J., R. W. Conners, C. A. Harlow, and G. S. Lodwick, "Towards Computer Analysis of Pulmonary Infiltration," Investigative Radiology, Vol. 13, August 1978, pp. 298-305.

10. Julesz, B., "Visual Pattern Discrimination," IRE Transactions on Information Theory, Vol. IT-8, February 1962, pp. 84-92.

11. Julesz, B., E. N. Gilbert, L. A. Shepp, and H. L. Frisch, "Inability of Humans to Discriminate Between Visual Textures That Agree in Second-Order Statistics-Revisited," Perception, Vol. 2, 1973, pp. 391-405.

12. Pavlidis, T., Structural Pattern Recognition, Springer-Verlag, 1977.

13. Chen, P. C. and T. Pavlidis, "Segmentation by Texture Using a Co-Occurrence Matrix and a Split-And-Merge Algorithm, Computer Graphics and Image Processing, Vol. 10, No. 2, June 1979, pp. 172-182.

14. Lendaris, G. G. and G. L. Stanley, "Diffraction-Pattern Sampling For Automatic Pattern Recognition," Proceeding of IEEE, Vol. 58, No. 2, February 1978, pp. 198-216.

15. Galloway, M. M. , "Texture Analysis Using Gray Level Run Lengths," Computer Graphics and Image Processing, Vol. 4, No. 2, June 1975, pp. 172-179.

16. Hsu, S. Y., "The Mahalonobis Classifier with the Generalized Inverse Approach for Automated Analysis of Imagery Texture Data," Computer Graphics and Image Processing, Vol. 9, No. 2, February, 1979, pp. 117-134.

17. Mitchell, O. R. and S. G. Carlton, "Image Segmentation Using a Local Extrema Texture Measure," Pattern Recognition, Vol. 10, No. 3, 1978, pp. 205-210.

18. Jensen, J. R., "Spectral and Textural Features to Classify Elusive Land Cover at the Urban Fringe," The Professional Geographer, Vol. 31, No. 4, November 1979, pp. 400-410.

19. Nakata, E., J. Iisaka, Y. Ishii, M. Imanaka, and Y. Miyazaki, "Application of Texture Analysis and Image Enhancement Techniques for Remote Sensing," Proceedings of the Twelfth International Symposium on Remote Sensing of Environment, (Ann Arbor, Michigan), April 20, 1978, pp. 1957-1971.

20. Nagao, M., T. Matsuyama, and Y. Ikeda, "Region Extraction and Shape Analysis in Aerial Photographs," Computer Graphics and Image Processing, Vol. 10, No. 3, June 1978, pp. 195-223.

21. Nagao, M. and T. Matsuyama, A Structural Analysis of Complex Aerial Photographs, Plenum Press, New York, New York, 1980.

22. Chien, Y. P. and K. S. Fu, "Recognition of X-Ray Picture Patterns," IEEE Transactions on Systems, Man, and Cybernetics, Vol. SMC-4, No. 2, March 1974, pp. 145-156.

23. Haralick, Robert M., "Statistical and Structural Approaches to Texture," Proceeding of IEEE, Vol. 67, No. 5, May 1979, pp. 786-804.

24. Caelli, T. and B. Julesz, "On Perceptual Analyzers Underlying Visual Texture Discrimination, I," Biological Cybernetics, Vol. 28, No. 3, 1978, pp. 167-175.

25. Caelli, T. and B. Julesz, "On Perceptual Analyzers Underlying Visual Texture Discrimination, II," Biological Cybernetics, Vol. 29, No. 4, 1978, pp. 201-214.

26. Julesz, B., E. N. Gilbert, and J. D. Victor, "Visual Discrimination of Textures with Identical Third-Order Statistics," Biological Cybernetics, Vol. 31, No. 3, 1978, pp. 137-140.

27. Pratt, W. K., O. D. Faugeras, and A. Gagalowicz, "Visual Discrimination of Stochastic Texture Fields," IEEE Transactions on Systems, Man, and Cybernetics, Vol. SMC-8, No. 11, November 1978, pp. 796-804.

28. Gagalowicz, A., " A New Method for Texture Fields Synthesis: Some Applications to the Study of Human Vision," IEEE _Transactions on Pattern Analysis and Machine Intelligence_, Vol. PAMI-3, No. 5, September, 1981, pp. 520-533.

29. Conners, R. W., "Discriminating Textures Which Have Identical Second-Order Probabilities Using the SGLDM", Remote Sensing and Image Processing Technical Report #402.82, Department of Electrical and Computer Engineering, Louisiana State University, 1982.

30. Conners, R. W., "Towards A Set of Statistical Features Which Measure Visually Perceivable Qualities of Textures," _Proceedings Pattern Recognition and Image Processing_, (Chicago, Illinois), August 8, 1979, pp. 382-390.

31. Conners, R. W. and C. A. Harlow, "Towards A Structural Textural Analyzer Based On Statistical Methods," _Computer Graphics and Image Processing_, Vol. 12, No. 3, March 1980, pp. 224-256.

32. Wertheimer, M., "Principles of Perceptual Organization," _Reading In Perception_, D. C. Beardslee and M. Wertheimer, Eds., D. Van Nostrand Co., New York, N.Y., 1958, pp. 115-134.

33. Julesz, B., "Cluster Formation of Various Perceptual Levels," _Methodologies of Pattern Recognition_, S. Watanabe, Ed., Academic Press, New York, 1969, pp. 297-315.

34. Mach, E., (1897) (Republished by Dover, New York, 1959), _Analysis of Sensations_.

35. Gibson, J.J., _The Perception of the Visual World_, Haughton-Mifflin, Boston, 1950.

36. Ohlander, Ron, Keith Price, D. R. Reddy; "Picture Segmentation Using a Recursive Region Splitting Method," _Computer Graphic and Image Processing_, Vol. 8, No. 3, pp. 313-333, 1978.

37. Riseman, E. M. and M. A. Arbib, "Survey: Computational Techniques in Visual Segmentation of Static Scenes," _Computer Graphics and Image Processing_, Vol. 6, No. 3, June 1977, pp. 221-276.

38. Harlow, C. A. and R. W. Conners, "Image Segmentation and Texture Analysis," _Proceeding SPIE Conference Image Understanding Systems II_, (San Diego, California), Vol. 205, August 29, 1979, pp. 30-41.

39. Coleman, G. B. and M. C. Andrews, "Image Segmentation by Clustering," _Proceedings of IEEE_, Vol. 67, No. 5, May 1975, pp. 773-785.

40. Chen, C. H., "On the Statistical Image Segmentation Techniques," _Proc. of the Pattern Recognition and Image Processing Conference_, Dallas, Texas, August 1981, pp. 262-266.

41. Chen, P. C. and T. Pavlidis, "Image Segmentation as an Estimation Problem," _Computer Graphics and Image Processing_, Vol. 12, No. 2, 1980, pp. 153-172.

42. Chen P. C. and T. Pavlidis, "Segmentation by Texture Using Correlation," _Proc. of the 5th International Conference on Pattern Recognition,_ Miami Beach, Florida, Dec. 1980, pp. 551-553.

43. Hughes, G. F., "On the Mean Accuracy of Statistical Pattern Recognizers," IEEE _Transactions on Information Theory,_ Vol. IT-14, No. 1, January 1968, pp. 55-63.

44. Foley, Donald, H., "Considerations of Sample and Feature Size," IEEE _Transactions on Information Theory,_ Vol. IT-18, No., 5, September 1972, pp. 618-626.

45. Morrison, D. F., _Multivariate Statistical Methods,_ McGraw-Hill, New York, 1967.

46. Zucker, Steven W., Demetri Terzopoulos, "Finding Structure in Co-Occurrence Matrices for Texture Analysis," _Computer Graphics and Image Processing,_ Vol. 12, No. 3, March 1980, pp. 286-308.

47. Duda, R. O. and P. E. Hart, _Pattern Classification and Scene Analysis,_ New York: Wiley Interscience, 1973.

48. Conners, R. W., M. M. Trivedi and C. A. Harlow, "The Segmentation of a Complex Urban Scene Using Texture Operators," Remote Sensing and Image Processing Laboratory Technical Report #401.82, Department of Electrical and Computer Engineering, Louisiana State University, March 1982.

FILMB